A 140 MHz Hardware Channel Emulator and FM Directional Wireless Channel Model for an Outdoor Environment

A thesis submitted to the
Graduate School of Natural and Applied Sciences

by

Ahmed Hossam MOHAMMED

in partial fulfillment for the
degree of Master of Science

in
Electronics and Computer Engineering

İSTANBUL
ŞEHİR
UNIVERSITY

This is to certify that we have read this thesis and that in our opinion it is fully adequate, in scope and quality, as a thesis for the degree of Master of Science in Electronics and Computer Engineering.
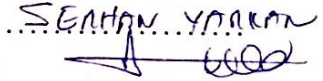
APPROVED BY:

Asst. Prof. Dr. Mehmet Kemal Özdemir

(Thesis Advisor)

Asst. Prof. Dr. Hakan Doğan

Asst. Prof. Dr. Serhan Yarkan

This is to confirm that this thesis complies with all the standards set by the Graduate School of Natural and Applied Sciences of İstanbul Şehir University:

DATE OF APPROVAL: 29 August 2016

SEAL/SIGNATURE:

Declaration of Authorship

I, Ahmed Hossam MOHAMMED, declare that this thesis titled, 'A 140 MHz Hardware Channel Emulator and FM Directional Wireless Channel Model for an Outdoor Environment' and the work presented in it are my own. I confirm that:

- This work was done wholly or mainly while in candidature for a research degree at this University.

- Where any part of this thesis has previously been submitted for a degree or any other qualification at this University or any other institution, this has been clearly stated.

- Where I have consulted the published work of others, this is always clearly attributed.

- Where I have quoted from the work of others, the source is always given. With the exception of such quotations, this thesis is entirely my own work.

- I have acknowledged all main sources of help.

- Where the thesis is based on work done by myself jointly with others, I have made clear exactly what was done by others and what I have contributed myself.

Signed: _Ahmed Hossam_

Date: _29 August 2016_

A 140 MHz Hardware Channel Emulator and FM Directional Wireless Channel Model for an Outdoor Environment

Ahmed Hossam MOHAMMED

Abstract

As the demand for higher data rates is increasing everyday, the behavior of certain channels ought to be more accurately described and modelled due to the higher sensitivity of the signal to the channel effects. For example, the knowledge of the directions from which the received signal arrives plays an important rule in the design of multiple-antennas systems. In this thesis, the general channel dynamics are studied. Several software and hardware wireless channel emulators are presented to show different approaches of modeling and emulating channels. Channel emulators are necessary for the performance assessment of the current wireless systems. In the thesis, we first present a software cluster based directional FM channel model for hilly outdoor environments. The model uses statistical and geometrical approaches to determine the time and directions from which different copies of the signal arrives. The model is based on the COST-259 model with modifications to better fit the FM band. A hardware emulator is also proposed and implemented in this research. The emulator can be used in testing the performance of communication systems on long time intervals due to the performance of filtering in time domain and avoiding the memory requirements of the frequency domain filtering. The emulator is simple due to the introduction of the Doppler effect in the RF domain, where the large number of time-domain filter coefficients are avoided. Moreover, the undesired distortions resulting from the down and up conversion of the signal taking place when the channel effects are introduced in software are avoided. The performance of the emulator is observed through the measurements performed on the developed circuits. It is observed that the channel emulator can indeed emulate a typical wireless channel. Thus, it is believed that the model and the emulator proposed in this thesis can help wireless system designers in assessing their system performance in lab environment conveniently.

Keywords: Channel emulator, Clustering, Spectrum Shaping Filters, FM

Dış Ortamlar için 140 MHz'de Donanımsal Kanal Emülatörü ve FM Yönsel Kablosuz Kanal Modeli

Ahmed Hossam Mohammed

Öz

Daha yüksek hızda haberleşme talebinin artması ile bazı haberleşme kanallarının hem doğru bir şekilde tanımlanması hem de daha doğru bir şekilde modellenmesi sinyallerin kanaldan dolayı etkilenmelerinden dolayı büyük bir önem arz etmektedir. Mesela, bir alıcıya gelen sinyallerin hangi yönden geldikleri çoklu anten sistemlerinin tasarımında büyük rol oynar. Bu tezde genel olarak kanal dinamikleri sunulmuştur. Farklı yazılımsal ve donanımsal kablosuz kanal benzetimleri, kanal modellemelerinde ve emülatörlerinde farklı yaklaşımların ne olduğu hususuna açıklık getirmek için sunulmuştur. Kanal emülatörleri günümüz kablosuz sistemlerinin performansını ölçmede gerekmektedirler. Bu tezde öncelikli olarak, yazılım tabanlı ve yönsel demetlerden oluşan bir FM kanalı modeli hafif dağlık alanlar için geliştirilmiştir. Bu yaklaşım istatistiksel ve geometrik yaklaşımları kullanarak gelen sinyalin yönünü ve gecikme zamanını hesaplamaktadır. Yazılım tabanlı bu yaklaşım için COST-259 modeli baz alındı ve fakat FM bandına uyması için değişiklikler gerçekleştirildi. Daha sonra bu araştırmada, donanımsal tabanlı bir kanal emülatörü belirlenen bir kanal tipi için önerildi ve implement edildi. Bu kanal emülatörü haberleşme sistemlerinin performansında kullanılabilir çünkü hem uzun süre boyunca zaman boyutunda filtreleme gerçekleştirebilir hem de frekans boyutundaki filtremeler gibi gereksiz miktarda bilgisayar hafızası gerektirmemektedir. Önerilen emülatör Doppler etkisini RF boyutunda gerçekleştirip, zaman boyutundaki bir sürü filtre katsayılarını kullanmadan implement ettiği için son derece basit bir yapıdadır. Bunlarla beraber emülatör, frekansı yükseltme (upconversion) ve düşürme (downconversion) işlevlerini gerektirmediğinden, bu işlevlerden dolayı meydana gelen bozulmalara da maruz kalmamaktadır. Geliştirilen emülatörün performansı tasarlanan devrelerle gözlemlenmiştir. Ölçümler sırasında emülatörün tipik bir kablosuz kanalı modellediği görülmüştür. Tüm bunlar bize gösteriyor ki bu tezde sunulan çalışmalar ile kablosuz sistem tasarlayıcıları geliştirdikleri sistemlerin performansını laboratuvar ortamında daha rahat gerçekleştirebilirler.

Anahtar Sözcükler: Kanal emülatörü, demetlenme, Tayf şekillendirici filtre, FM

Acknowledgments

I would like to express my most valuable appreciation to my advisor Asst. Prof. Mehmet Kemal Özdemir for his support, contribution, patience, and guidance. Without his patience and sacrificing hours for me, this thesis will never be written.

Special thanks to Asst. Prof. Dr. Hakan Doğan and Asst. Prof. Dr. Serhan Yarkan for being committee members of my thesis.

Finally, I wish to thank my parents, my sisters, and my friends for their support and encouragement throughout my study.

Contents

List of Figures

List of Tables

Abbreviations

MPC	**M**ulti**p**ath **C**omponent
LOS	**L**ine **O**f **S**ight
NLOS	**N**on-**L**ine **O**f **S**ight
PDP	**P**ower **D**elay **P**rofile
ISI	**I**nter**s**ymbol **I**nterference
CIR	**C**hannel **I**mpulse **R**esponse
IO	**I**nterfering **O**bject
AOD	**A**ngle **O**f **D**eparture
AOA	**A**ngle **O**f **A**rrival
DOD	**D**irection **O**f **D**eparture
DOA	**D**irection **O**f **A**rrival
BA	**B**ad **U**rban
HTR	**H**illy **Terrain R**egion
VHF	**V**ery **H**igh **F**requency
RVC	**R**everberation **C**hamber
SOS	**S**um **O**f **S**inusoids
SSF	**S**pectrum **S**haping **F**ilter
FIR	**F**inite **I**mpulse **R**esponse
IIR	**I**nfinite **I**mpulse **R**esponse
SAW	**S**urface **A**coustic **W**ave
IDT	**I**nter**d**igital **T**ransducer
ACF	**A**uto**c**orrelation **F**unction
PSD	**P**ower **S**pectral **D**ensity
OFDM	**O**rthogonal **F**requency Division Multiplexing
CP	**C**yclic **P**refix

GFDM   **G**eneral **F**requency **D**ivision **M**ultiplexing

CDF   **C**umulative **D**istribution **F**unction

PWM   **P**ulse **W**idth **M**odulation

MIMO   **M**ultiple **I**nput **M**ultiple **O**utput

BS   **B**ase **S**tation

MPG   **M**ulti**p**ath **G**roup

AWGN   **A**dditive **W**hite **G**aussian **N**oise

ADC   **A**nalog-to-**D**igital **C**onverter

DAC   **D**igital-to-**A**nalog **C**onverter

IFFT   **I**nverse **F**ast **F**ourier **T**ransform

FFT   **F**ast **F**ourier **T**ransform

ASK   **A**mplitude **S**hift **K**eying

Chapter 1

Introduction and Motivation

Centuries ago, wireless communication was done through non-electrical techniques for transfer of information such as smoke signals and signal flags in maritime operations. Wired electrical telecommunication systems started appearing in the 1830s. The electric telephone was invented in the 1870s, and in 1878 and 1879 the first commercial telephone services were released. Alexander Graham Bell held the master patent for the telephone where all other patents for electric telephone devices were after this master patent. The first telephone company, the Bell Telephone Company was established by Alexander Graham Bell and Gardiner Greene Hubbard in the United States. In 1880, Bell and co-inventor Charles Sumner Tainter conducted the first wireless telephone call via modulated lightbeams projected by photophones where a wireless voice telephone message was transmitted from the roof of the Franklin School to the window of Bell's laboratory, some 213 meters away. Guglielmo Marconi could then perform many outdoor wireless transmission experiments where the transmission distance was substantially increased. Shown in Fig. 1.1 is the structure of his Radio system [1].
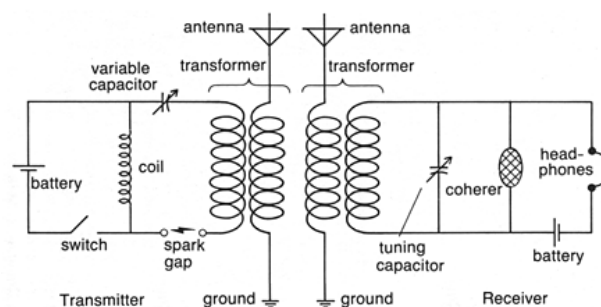
FIGURE 1.1: Marconi's Radio System [1]

Electrical wireless communication systems have been undergoing through huge enhancing developments throughout the past few decades. Modern wireless communication systems started initially with the transmission of the analog voice. The first generation of wireless mobile telecommunications (1G) system was introduced in the 1980s [8]. There, voice was transmitted without any digitization, and hence it was transmitted as an analog signal. Digitizing the signal increases the system's immunity towards the noise introduced in the channel. Besides, there was no unified standard among all the 1G system vendors. This did not serve the compatibility of a certain manufacturer's mobile equipment with a network developed by another manufacturer. Thus, only mobile equipments belonging to the same network vendor could communicate with each other. In the end, 1G systems did not offer handover between different base stations. This did not offer the user the mobility luxury across different base stations without having the call dropped. Hence, there showed up the need to design a new unified standard that offers handover. These new systems -starting from 2G- offer the transmission of both voice and data where the digitizing of the signal takes place.

Enhancements in the digital systems were focused on modifying the modulation scheme that would result into the maximum possible data rate and that would best combat the undesired channel effects and noise. It should be noted that the higher the desired data rate becomes the more distortion due to a certain channel on the transmitted signal occurs.

Starting from 2G systems till the newly developed wireless generations, the main aim was to design a system that delivers higher data rates as compared to the previous ones. Therefore, as we advance in wireless generations, the wireless channel models should be more precise and accurate about the description of the behavior of the real channel as the high data rate signals get more sensitive to the channel effects.

Newly developed systems deploy Multiple Input Multiple Output (MIMO) technique in the transmission of data in order to multiply the channel capacity by exploiting the multipath propagation [9]. Simply explaining the intuition behind the concept of MIMO technique, different data signals are being sent on the same channel at the same time through different antennas. This leads to the smearing of the received signal due to the interference between the transmitted data symbols. However, multiple antennas are utilized at the receiver side as well. Each of those receiving antennas gets a different

version of the smeared signal due to the variance in the channel effect on each of the transmitted data symbols. This divergence in the channel effects arises from the distinction between each path taken by each data symbol from its transmitting antenna to the multiple receiver antennas. Fig. 1.2 [2] below is a simple figure illustrating how the multiple receiver antennas receive different waveforms due to the multipath propagation environment.
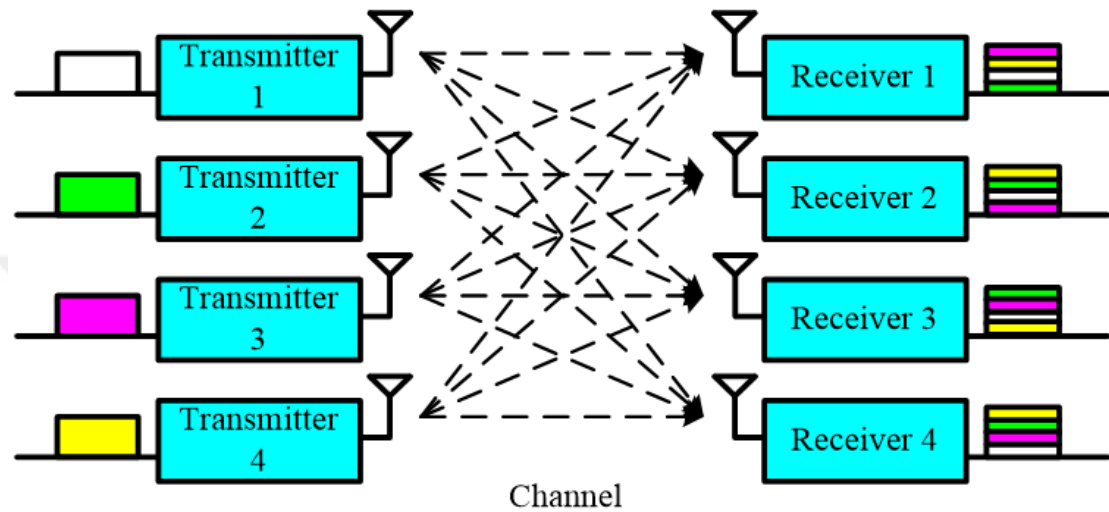
FIGURE 1.2: Illustrative figure of the MIMO concept [2]

The multiple received signals undergo complex signal processing in order to recover the original transmitted symbols. This technique as shown takes advantage of the variance in the multipath propagation of the channel through space diversity. Thus, it is important to know the direction from which different signals are received. Hence, not only a channel model, that describes the channel in terms of delay spread, rate of change of the channel effect (Doppler effect) and noise, is important for the testing of the system efficiency, but also the directionality of the wireless channel must be taken into consideration for the MIMO deploying systems [9].

1.1 Importance of Channel Emulators

As the new applications are getting more eager for higher data rates, new products are presented to the market. These newly developed products should be examined through several tests before they get introduced out for the market. Thus, it is required to check

the performance of the products in realistic channel scenarios where the efficiency of the products can be determined. Implementing channel tests in the field is a costly and time consuming process and in some cases like satellite communication it might not even be feasible. Therefore, there shows up the need to design wireless channel emulators that introduce the widely varying channel effects to the signal in a laboratory environment. With a large variety of the communication system applications, this has been a clear necessity. For instance, testing communication systems for a high speed train or an air vehicle is a challenging task. As the arrangement of an air vehicle and getting the required permissions and licenses is a long process, the products development time is negatively affected.

Channel emulators can provide a testing platform for realistic channel scenarios. Especially, for long range and/or high speed communication systems, implementing realistic test scenarios in laboratory environment is very crucial. Channel emulators can be used to imitate realistic different channels.

A communication channel introduces power loss, in addition to time and frequency dispersion on the signal. Moreover, additive Gaussian noise adversely affect the information signal. The impact of those effects vary depending on the communication environment, carrier frequency and bandwidth of the signal. If the system is not designed to be robust against those effects, a poorly performing system will be delivered.

Shown in Fig. 1.3 is a thorough framework of a communication scenario where the performance of the designed communication system can be assessed at the receiver side in a lab environment with the help of the Emulator.
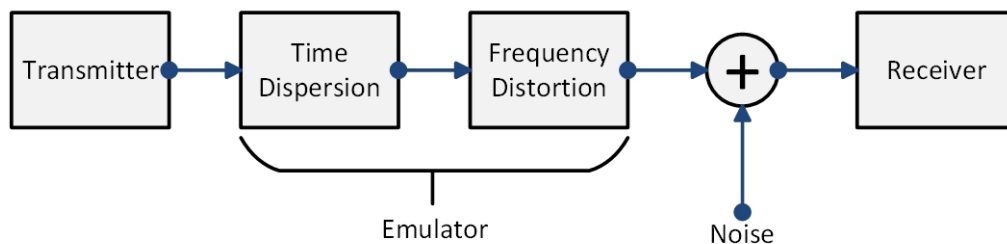
FIGURE 1.3: Overall structure of a communication scenario.

1.2 Behavior of Wireless Channels

The behavior of a wireless channel has to be known in order to be able to emulate it. This behavior at a certain frequency can be known "accurately" only via real measurements in different types of environments whether indoor or outdoor environments. However, performing measurements might be a time and money consuming task. Hence, another approach to predict the behavior of the channel is through the performance of ray tracing simulations that still requires very precise information about the surrounding environment [10]. Ray tracing simulations in general are more efficient in indoor simulations because the surrounding environment becomes much more simpler and easier to model as compared to the vast outdoor environments where the detailed modeling of such a wide surrounding with large number of parameters becomes infeasible. Once the behavior of the wireless channel is determined, it can then be described statistically such as the famous Saleh and Valenzuela model [11]. The statistical model may have some parameters that might change in order to fit a wider range of wireless channels (different frequencies or different environment types). These statistical models may also include geometrical approach as the case in the COST 259 model [12].

In this thesis, we first underlie the main parameters of a wireless channel and then we develop a hardware based wireless channel emulator that reflect these main parameters. Specifically, the purpose of this study is to provide wireless channel models for low frequencies, but in order to do that the wireless channel behavior and effect over the signal has to be well studied.

Shown in Fig. 1.4 is the comprehensive methodology for the emulation of a certain channel. Understanding the behaviour of the channel serves in providing a model capable of describing that behaviour. The provided model might be statistical. Based on this model, a certain predefined realization of that channel can be then emulated.
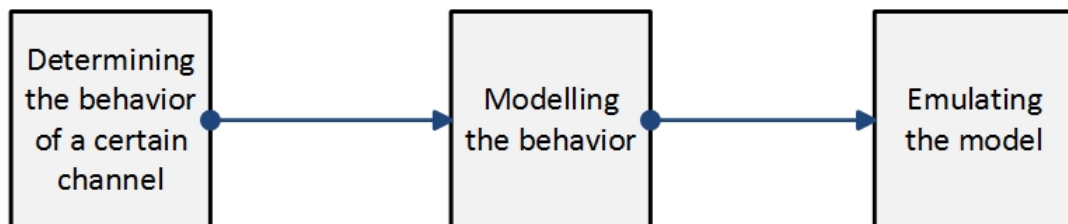
FIGURE 1.4: Certain wireless channel emulation steps.

The outline for the rest of the thesis is as follows: Chapter 2 will explain the wireless channel behavior. Chapter 3 will then give a brief overview over the different hardware and software channel simulators that were utilized. A comparison between introducing the channel effects to the signal in hardware and software will also be held. Chapter 4 will present a software FM channel model proposed by the authors. Chapter 5 includes the implementation of a hardware channel emulator at 140 MHz, while Chapter 6 concludes the work and predicts the future work.

Chapter 2

Dynamics of Wireless Channels

The previous chapter included the motivation lying behind our work. It illustrated the significance of modeling the wireless channels so as to provide a basis on which a wireless communication system performance can be assessed. This chapter will include a brief explanation of the wireless channel behavior and the way it affects the transmitted signal.

2.1   Signal Transmission through Wireless Channels

It is widely known that when a signal is transmitted over a wireless channel, it spreads in different directions through the surrounding depending on the antenna radiation pattern. Each of those spread copies of the signal is called a Multipath Component (MPC). Each of those MPCs make its own way till it reaches the receiver. Some MPCs may reach the receiver directly from the transmitter. Those MPCs are known as Line-of-Sight (LOS) components. The rest of the MPCs suffer reflections from different Interfering Objects (IOs) before reaching the receiver. These MPCs are known as Non-Line-of-Sight (NLOS) components. According to [11], MPCs do get received in the form of what is known as clusters. A cluster is formed by a group of MPCs leaving the transmitter within a small range of departure solid angles, and then arriving at the receiver within a small range of arrival solid angles. The group of MPCs will typically arrive at the receiver within a small range of time interval between the arrival time of the first and the last MPC within a given cluster. Therefore, the reception of a signal in a multipath wireless channel comes in the form of a number of received clusters. Each of those clusters has

its own delay spread, Angle-of-Departure (AOD) and Angle-of-Arrival (AOA) as shown in Fig. 2.1. It is clear from the figure that the receiver receives 3 clusters, each of them containing several MPCs. To understand it in a better way, it can be imagined that each of those large arrows (representing clusters) consists of thin arrows (representing MPCs) as shown in the figure. Each and every MPC in general is characterized by its Direction of Departure (DOD) and Direction of Arrival (DOA) angles as well as by their time of arrival. Each cluster has its main MPC, so when a cluster arrival time or directionality (cluster's features) is mentioned, it refers to the features of the main MPC of that cluster. The main MPC of each cluster is assumed to be the first one received by the receiver among all the other MPCs of the same cluster. Each cluster has its visibility area (omitting the third dimension) in the region of operation. Therefore, according to Fig. 2.1 the receiver lies inside the visibility regions of three clusters. The LOS cluster has no blocking IO, while other NLOS clusters are perturbed by one or more IOs. As can be seen in Fig. 2.1, one cluster is perturbed by a mountain while another one is disrupted by a building.
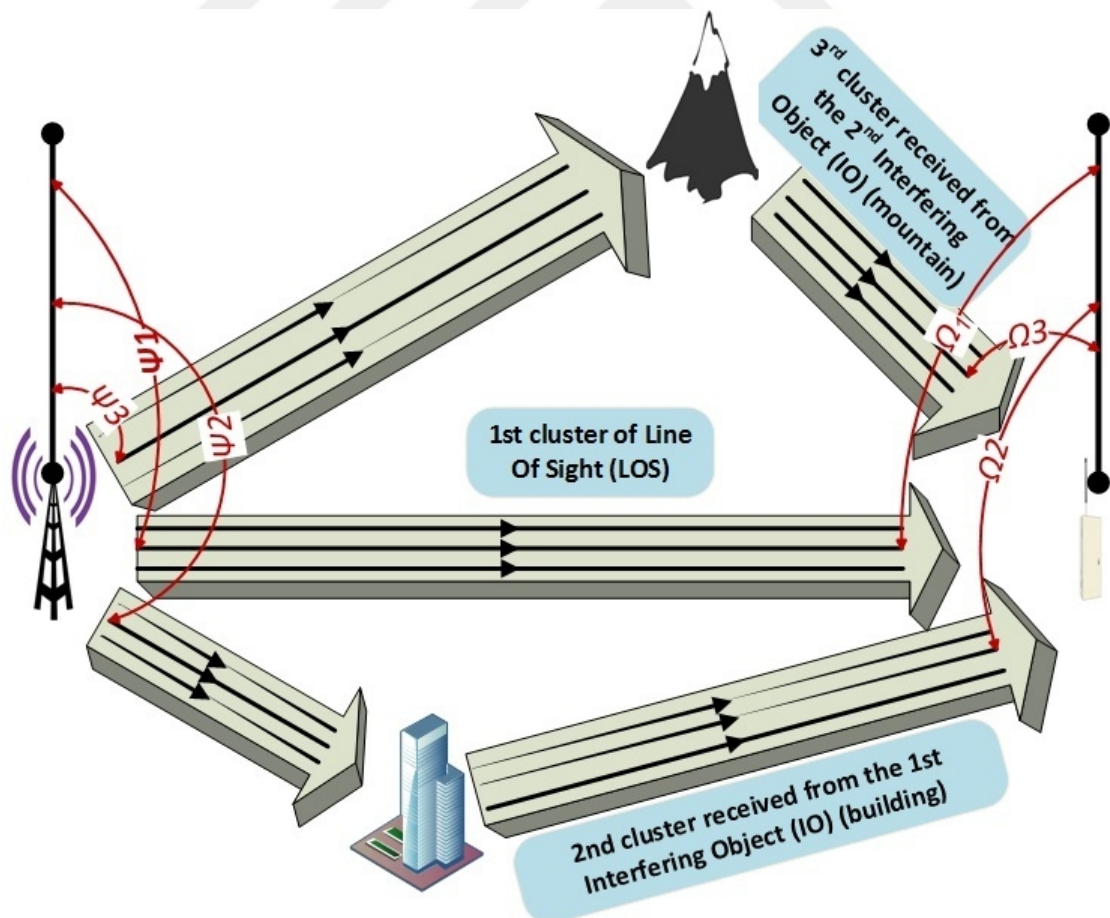
FIGURE 2.1: Illustrative Figure of clusters concept.

Note that the total channel delay spread is determined based on two factors: the time at which each cluster begins and the delay spread within each of those clusters. Power Delay Profile (PDP) gives an indication for the intensity of a signal received through a multipath channel as a function of time delay. The time delay is the difference in travel time between multipath arrivals. Thus, the propagation delay between the transmitter and the receiver is usually not included in the PDP and hence, the first received MPC starts at time zero on the PDP graph.

Fig. 2.2 [3] shows the reception of many clusters where the received power within each of those clusters generally decays exponentially as time advances. This is believed to be the general case as adopted in many of the reviewed studies [11–13] whether in an indoor or an outdoor environment. The PDP shown is possible for an indoor environment with a high frequency of operation. This is anticipated since the delay spread is not too large (in the order of nanoseconds). High frequencies suffer large attenuation and in the case of indoor environments, IOs are usually in the vicinity of the receiver. This makes it not very probable to have a certain cluster that travels to a very far IO and come back to the receiver. A table of measurements in Chapter 3 will show that relatively lower frequencies of operation in outdoor environments result in delay spreads in the order of microseconds.
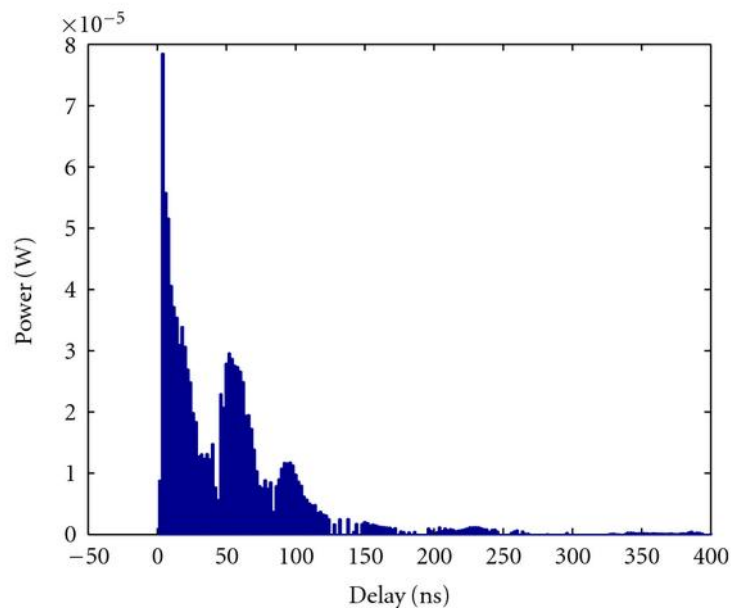
FIGURE 2.2: Illustrative figure showing the exponential power decay within each cluster with the advance of time. [3]

Sometimes, there arises the need to discretize the channel into N taps or distinct bins. All of MPCs received within a bin are unresolvable by the receiver and are represented by a single tap. The maximum possible sampling period of the channel depends on the bandwidth of the signal. As the signal bandwidth increases, the maximum allowed sampling period decreases. The physical explanation of this is as follows: An increase in the bandwidth of the signal means a corresponding decrease in the symbol duration. This makes the signal more sensitive to the time distortion caused by the arrival of relatively late MPCs that might further cause Inter-Symbol Interference (ISI) where one symbol interferes with subsequent symbols. And hence, to emulate the channel in a better way, higher sampling rate is required in order to take into consideration more channel effects by reducing the sampling period.

Typically, the number of received MPCs is very large. And hence, in order to determine how the PDP will look like, the bandwidth of the system has to be taken into consideration. For instance, when the system bandwidth is too large, small sampling period becomes essential. In this case, the channel may look continuous since large number of MPCs are received within a short interval with a high resolution. The PDP shown below in Fig. 2.2 is a possible example. On the other hand, for a system with smaller bandwidth, such high resolution becomes unnecessary and therefore, more MPCs arriving within the longer sampling period are represented by a single tap. As a conclusion, the more the bandwidth of the signal becomes, the more the PDP of a certain channel appears to become continuous due to to the increase in the number of resolvable taps.

Fig. 2.3 shows a discretized PDP. This kind of discretization becomes very useful when the channel effects are introduced to the signal in software. There, the signal is discretized and the channel effect is introduced to the signal in software with the help of a processor.
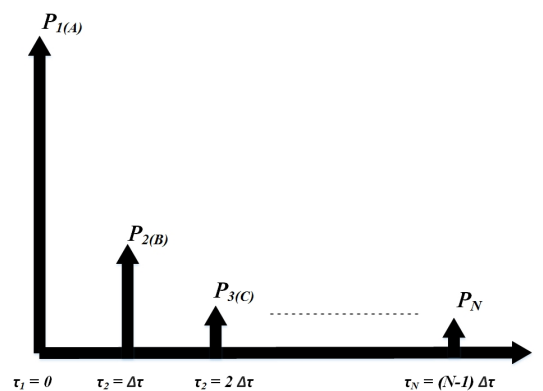
FIGURE 2.3: PDP of an N tap channel with equal spacing of $\Delta\tau$.

Note that ISI becomes very significant when the time distortion is too large. Small time distortion may just lead to the addition of different copies of the same symbol with each other. These copies may add constructively or destructively when there is a phase difference. When the delay spread is large as compared to symbol duration, copies of different symbols will start adding together. To overcome that, complex equalization needs to be performed at the receiver side to remove the ISI effect. But first of all, the ISI effect has to be accurately modelled in order to be able to remove that effect. Fig. 2.4 [4] shows the overlap that happens in time domain between different copies of different symbols where A, B and C are three different channel taps.
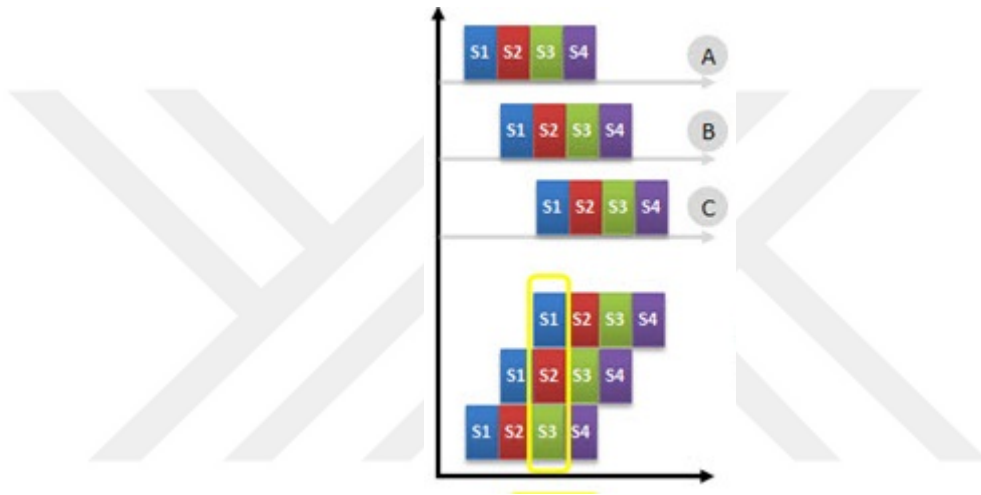
FIGURE 2.4: Illustrative figure of ISI effect [4], where A, B and C represent a 3-taps channel as indicated in Fig. 2.3.

2.1.1   Mathematical Channel Model

According to the previous explanation and regardless of the clusters concept, an N-tap channel can be represented by

$$h(t, \tau) = \sum_{n=1}^{N} c(t)\delta(\tau - \tau_n) \tag{2.1}$$

where $h(t, \tau)$ is the Channel Impulse Response (CIR) that describes the behavior of a certain channel when a unit impulse is being sent, $c(t)$ is the complex amplitude of the nth tap, δ is the Kronecker delta function and τ_n is the time at which the nth tap gets received as compared to the first tap that is assumed to be received at zero.

The delay spread of the channel is considered to be a measure for the channel selectivity in the frequency domain. The signal is convolved with the CIR in the time domain that corresponds to a multiplication in the frequency domain. For a single-tap channel, the frequency response of the channel $H(f)$ is constant for all frequencies f. Therefore, for such a case the channel is considered to be flat for all the frequencies of the signal where it affects all the frequency components of the signal with the same amplitude. However, wireless channels are not single-tap channels typically. As the delay spread of the channel increases the channel becomes more selective, affecting different frequency contents of the signal with different amplitudes. This selectivity requires equalization of the channel at the receiver. The bigger the delay spread gets, the more complex the equalization process becomes. The coherence bandwidth is defined as the bandwidth through which the channel is considered to be flat. Thus, the coherence bandwidth of the channel decreases with the increase of the delay spread. In order to make good equalization at the receiver, a good channel estimate should be done where the delay spread of the channel has to be well modelled. This is one of the points that shows the significance having a good channel model.

2.1.2 Doppler Effect in Wireless Channels

The PDP is typically derived by averaging the received power over a local area. This PDP is then sampled into N taps and the channel delay spread is calculated through the PDP. Within that local area the CIR changes from one position to another. This change is only in the form of a change of the complex amplitudes of the channel taps $c(t)$, not in the form of an increase or decrease in the number of taps itself. This comes from the assumption that the channel does not change dramatically within a small local area. To sum it up, within a local area, the PDP is constant and so is the corresponding delay spread while the CIRs differ from one location to another by the change in the complex amplitude of the fixed channel taps. Hence, $c(t)$, is the only function of time t in the equation as shown. This change with time is due to the motion of the transmitter, receiver or one or more of the surrounding IOs. This motion results into the change of the CIR within the local area. And therefore the complex amplitudes of the channel taps change with time. The amplitude of the channel taps within a local area is agreed widely to be Rayleigh distributed for the NLOS channel taps and Ricean distributed for

the LOS channel tap if exists [12]. This effect of change in the CIR with time is known as the Doppler effect.

Note that the receiver might be still in its position while the CIR changes due to the motion of the transmitter and/or the surrounding IOs. Therefore, the change of the complex amplitude of a certain tap in the CIR is related to the "relative" velocity of the receiver with respect to the direction from which that tap is received.

In order to study the Doppler effect from another perspective, let's consider it in terms of frequency domain. In frequency domain, the Doppler spread refers to the frequency shift that happens to the received signal where some frequency bands might be received at the receiver side without originally being transmitted at the transmitter side. That is, the receiver is receiving some data that had not been part of the sent signal. Fig. 2.5 [5] simply shows that the receiver whose direction of motion is against the direction of arrival of the signal (the one on the right) is actually receiving the signal with a frequency higher than the original one. The receiver on the left is in contrast with that case.
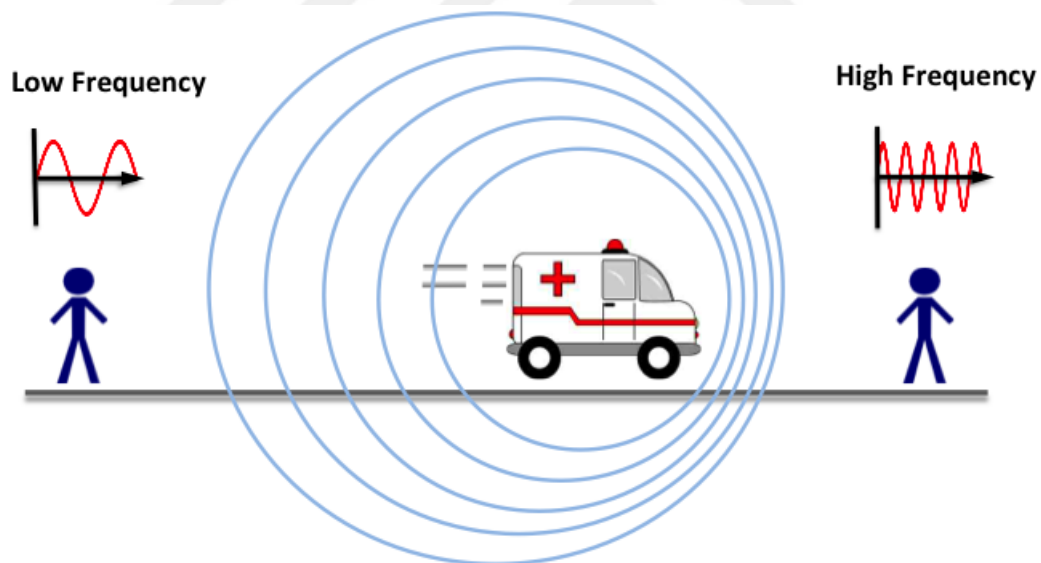
FIGURE 2.5: Frequency shift of the received signal due to the relative velocity of the receiver with respect to the direction of arrival of the signal [5].

If a tap is received from a direction perpendicular to the relative velocity of the receiver, there will be no frequency shift, meaning as if there is no motion at all. The received frequency will be the same as the transmitted one then. Thus, the Doppler spectrum varies with the movement scenario in the environment where each channel delay tap

may have its own unique Doppler spread depending on the direction of movement of the receiver with respect to the direction from which the tap is received.

Generally, it is intuitional to expect a relatively fast change in the CIR when the relative velocity of the receiver is high, while the change in the CIR is slower when the velocity is less. The coherence time of the channel is defined as the time over which the channel is considered to be constant.

In a design of a system, it is important to have the duration of any transmitted symbol to be less than the coherence time of the channel. Achieving this condition makes the equalization of the channel effect during a single symbol a simpler process since the channel is considered to be constant along the whole symbol duration. The receiver makes a channel estimation as a first step in order to be able to equalize the received signal. Since the symbol duration is shorter than the coherence time of the channel, the channel estimate that the receiver has is not expected to change dramatically along the whole symbol duration and therefore, this single estimate is enough to make a good equalization while no other estimate needs to be done within the same symbol. Other channel estimates might be needed after the coherence time of the channel. This is another point showing the importance of having a good channel model so that the system design suits the given channel conditions. The coherence time shall be well modelled and accordingly the symbol duration should be determined.

2.2 Chapter Conclusion

This chapter explained the basic concepts that shall be adopted for the understanding of the wireless channel effect on the transmitted signal. It also illuminated the importance of having a good channel model for the sake of designing a communication system that performs well in a given channel. Thus, channels have to be accurately described by the model to result into a good performing system and to successfully assess the performance. The following chapter will present the literature reviewer. It will present an overview of different software channel models. Some hardware channel emulation techniques will also be discussed. Furthermore, the strengths and the weaknesses of software and hardware approaches will be provided as a comparison between them. Finally the need for this study will be stressed once more.

Chapter 3

Literature review

After the previous chapter has explained the physical behavior of a wireless channel and the influence it has over the transmitted signal in both time and frequency domain, this chapter shall introduce different models in the literature that describe the wireless channel behavior. The introduction of the channel effect to the signal can be done either in hardware or software. However, most of the available studies propose software statistical simulators rather than hardware channel emulators. A comparison between software and hardware implementations will be held to understand the pros and cons within each of the implementations.

3.1 Software Channel Models

Some of the famous cluster-based software wireless channel simulators will be briefly discussed in this section. It is to be noted that different models are deployed for different ranges of frequencies and for different environment types.

As mentioned earlier, the cluster concept was firstly introduced in [11]. This model was based on some indoor measurements. It assumed the clusters and the MPCs within a cluster form Poisson arrival processes and they also have exponentially distributed inter-arrival times. The amplitudes of the taps are modeled as Rayleigh random variables whose variances decay exponentially with cluster delay as well as excess delay within a cluster. However, this model does not provide the directionality of the arriving MPCs.

Determining the DOA of the MPCs play a crucial role in modern systems that deploy MIMO technique as stated before.

Hence, new models that take the DOA of the MPCs into consideration were developed in order to model the channel. The COST259 [10, 12] models the AOD and AOA of different MPCs via geometrical means. The location of the IO of a certain cluster is drawn from a 2-directional Gaussian distribution with its mean at the center of the visibility region of the corresponding cluster. These visibility regions are previously determined where the whole region of operation is divided into many clusters visibility areas. After determining the IO location, the AOD, AOA and the arrival time of the main MPC are determined through simple geometry. The shadowing, delay spread, azimuth angular spread and elevation angular spread of that cluster are then modelled as log-normal distributions where the shadowing, delay spread and azimuth angular spread are correlated together while the elevation angular spread is independent. MPCs delays and angles are then uniformly distributed within the cluster's spreads. The distribution does not have to be uniform as long as the resulting amplitude of each tap in the CIR is Rayleigh distributed. However, large number of MPCs should be generated within each bin in order to guarantee that the amplitude of their sum results into a Rayleigh-distributed amplitude channel tap. The COST259 model serves a wide range of frequencies and it can work for different environment types by changing different parameters. This gives it an advantage in terms of flexibility. However, it does not work for the FM band.

The next chapter will be dedicated for the description of an FM software channel model proposed by the authors. Thus, we will cut software techniques in this chapter short.

3.2   Hardware based Channel Emulators

The main two challenges in the process of emulating the wireless channel in hardware is the introduction of the delay taps and the Doppler effect under the assumption of previously known channel delay taps and the Doppler effect for each tap.

In the previous work it was found that delays were introduced to the signal through simple cables extension [14]. Although this approach is simple, it does not seem to be very practical due to a couple of reasons. Being able to get the transmission line that results into the exactly desired delay value is not an easy task since most of the

commercially available RF cables have standardized lengths. Therefore, there is no wide variety of different cables lengths to choose from. This does not offer high flexibility. Moreover, achieving large delays lead to the utilization of very large number of cascaded cables that makes the hardware emulator device too bulky and expensive as well. For instance, to generate a short delay of 333 ns, 100 m cable is needed. Besides, cascading large number of cables result into a large loss due to the presence of large number of connectors. The single connector loss is not something that is to be neglected. Thus, the cables extension approach is not a feasible one especially when relatively small frequencies are required to be modeled since the typical delay spread values for small frequencies is very large for some outdoor environments. This might in turn require cables in terms of hundreds and even thousands of meters in length.

One of the purposes of this thesis is to develop a hardware RF channel emulator that provides large flexibility in the supported delay values. Hence, the literature has been surveyed extensively to check the different delay spread values at different frequencies of operation and for different environments. Shown below in Table 3.1 is the summary of the literature survey concerning typical delay spread values for different operational frequencies and environment types. Some of the separation distances between the transmitter and the receiver at which those typical delay spread values were measured are also in the table. The recognition between different environment types followed the convention in [12] where the detailed description of the different environment types is as follows:

- *Urban:*

  Cities and towns where the buildings are of nearly uniform height and density.

- *Bad Urban (BA):*

  Cities with nonuniform distributed building heights or densities such as high-rise metropolitan centres and cities with large open areas like rivers, lakes or parks.

- *Suburban:*

  Where buildings are typically few, such as farmlands, fields and forests.

- *Hilly Terrain Region (HTR):*

  Similar to suburban areas, but with some large heights such as hills or mountains.

TABLE 3.1: Typical delay spread values for different frequencies of operation in various environment types at different separation distances between the Transmitter and the Receiver.

Frequency	Environment type	Typical Distance	Delay Spread
2 GHz	Urban/BU	1000 m	median: 0.4 μsec [12]
2 GHz	Suburban/HTR	1000 m	median: 0.1 μsec [12]
1.8 GHz	Urban	0.2 - 1.1 Km	mean: 1.2 μsec [15]
1.8 GHz	BU	0.9 - 1.6 Km	mean: 1.7 μsec [15]
1.8 GHz	Suburban	0.3 - 2 Km	mean: 0.5 μsec [15]
910 MHz	Urban	-	mean: 1.3 μsec max: 3.5 μsec [16]
910 MHz	Suburban	-	averaged extreme case: 1.96 - 2.11 μsec [16]
900 MHz	Urban	-	typical: 2 - 3 μsec [17]
900 MHz	HTR	-	typical: 5 - 7 μsec [17]
892 MHz	BU	-	worst case: 10 - 25 μsec [16]
210 MHz	HTR	-	medium delays: 10 - 20 μsec [18]
145 MHz	HTR	-	typical: 25 μsec [19]

Regardless of the separation distance and the environment type, it is obvious from the above table that there is a general inverse proportionality between the frequency of operation and the measured delay spread values. It is also expected to have such a relation, where the propagation loss decreases with the decrease of the frequency of operation. Therefore, as the frequency of operation decreases, there becomes a higher chance for the signal to survive till it impinges with a relatively far IO and reflects back to the receiver. The purpose of this thesis is to emulate the challenging wireless channels rather than the easy ones to prove that the proposed design is feasible for most of the wireless channels. Thus, we choose our hardware emulator to operate at low frequency of operation, namely 140 MHz that lies in what is known as the Very High Frequency (VHF) band. The naming here is just to follow the naming standard, though this band is small as compared to the other bands utilized for the contemporary digital

transmission systems. Hence, the VHF wireless transmission systems are to be designed taking into consideration that they have large delay spread values as compared to the rest of the digital systems. Therefore, for the VHF channel emulators, other feasible delay approaches must be utilized to overcome the previously mentioned problems.

One of the challenges for the hardware based channel emulators is the introduction of the effect of Doppler, which is due to the motion of the communicating devices. Different articles have been reviewed to check different techniques for the introduction of the Doppler effect. For instance, in [20] the idea of the introduction of the Doppler effect via reverberation chamber (RVC) was proposed. The idea was to feed the signal into the RVC. It is simply nothing but a metallic box in which stirrers are being fixed and then receiving the resulting signal. The resulting spectrum changes with the change in the number of the rotating stirrers as well as their speed. The technique is considered to be simple since the Doppler effect introduction is done via mechanical approach. Thus, it arises from the theoretical definition of the Doppler effect itself that results from the motion of the Transmitter, Receiver, or the surroundings. This motion is introduced via the rotating stirrers. In spite of the simplicity of the technique's concept and the ease of its understanding, it is considered to be impractical for the following reasons:

1. The large bulky nature of the RVC block.

2. The difficulty of inserting new stirrers that doesn't make it flexible enough.

3. The unintentionally generated multipaths caused by the impingement of the waves with the walls of the RVC. These reflected multipaths are also subjected to the Doppler effect caused by the motion of the stirrers. This makes the RVC approach for the generation of a specific Doppler spectrum infeasible since the process is fully out of control.

Two other main approaches are widely known for the generation of the fading waveform. The first one -known as Sum of Sinusoids (SOS)- was firstly proposed in [21]. It was simplified in [22] later. The basic idea relies on the superposition of a number of sinusoids with equal amplitudes and uniformly distributed phases in order to generate the fading channel waveform. There were several attempts for further improvement of the technique in [23], [24], and [25]. This technique is computationally heavy due to the large number of expensive $sin()$ function calls required in the simulation as mentioned in [26].

The second utilized approach is the filter-based approach. In [27], the basic idea is to pass two parallel independent streams of independent Gaussian distributed samples through two Spectrum Shaping Filters (SSFs). The input sequence has almost a flat frequency spectrum while the SSF is designed in a way such that the output is characterized with the desired spectral power density when the input has a flat power spectrum.

As compared to the SoS-based method, the filter-based approach is much trickier in the design and the implementation. This is due to the stability issue of the SSF that has to be carefully checked. On the other hand, filter-based fading simulation has several advantages over the SoS-based method. First, it is more flexible since it is possible to simulate a wide range of power spectral densities with the filter-based method. Besides, high level of statistical accuracy can be achieved [28].

The filtering process can be carried out either in the time or frequency domain. In the frequency domain, independent Gaussian samples are multiplied by the absolute of the square root of the desired Doppler power spectrum. Inverse Fast Fourier Transform (IFFT) is then applied to the resulting spectrum to obtain the time fading sample series [29]. The resulting fading sequence is still Gaussian thanks to the linearity of the IFFT. Hence, the resulting series will have the desired spectrum. One major drawback of the IFFT method is its block-oriented nature. This implies the generation and storage of all fading samples coefficients before data is processed by those channel coefficients. This requires significant memory and hinders unbounded continuous transmission. Unlimited continuous transmission is usually preferred in long running characterization applications such as hardware fading simulation, which is the case in this study.

Therefore, we are left with the filtering in the time domain that can be done either through finite impulse response (FIR) filters [30, 31] or infinite impulse response (IIR) filters [26, 32]. When implementing fading channel simulators using FIR and IIR filters, it is important to note that the degree of the FIR filter is directly proportional to the time span of the truncated signal held in the filter. Moreover, increasing the filter order offers the luxury of decreasing the minimum Doppler frequency shift that can be accurately achieved. Note that the Doppler shift is typically much smaller than the frequency of operation in real cases due to the small relative velocity of the receiver with respect to the received channel tap. This leads to the requirement of designing a filter whose passband is extremely narrow with a sharp cutoff and very large attenuation in the stopband.

This in turn requires a high-order FIR filter. IIR filters can typically meet the same specifications with fewer hardware resources as compared to FIR filters. IIR filters can offer steeper frequency roll-offs for a specific filter order as compared to an FIR filter [33]. FIR filters are inherently stable because they have no feedback. Therefore, extra attention must be drawn to the stability of the designed SSF when it is desired to reduce the computational complexity by utilizing IIR filters rather FIR ones.

3.3 Pros & Cons of Hardware and software emulating techniques

In the literature, most of the proposed channel emulators generate the effects of realistic channel conditions with some baseband processing techniques via the help of a processor. Although the implementation of these statistical models in software programs is flexible since the delays of the channel taps change accordingly, the simulation is done in the baseband. Therefore, they require the down conversion of the data, digitizing, convolving with the baseband channel, introducing Doppler effect, adding the noise followed by an up conversion. These down and up conversions introduce additional undesired hardware distortions such as Analog-to-Digital Converter/Digital-to-Analog (ADC/DAC) quantization errors. These distortions are added to the signal beside the desired channel distortions [34]. Besides, having real-time software simulations is a challenging task. Hence, there arises the need to introduce the channel effects on the signal in real-time via hardware without having to get bothered with the undesired distortions. There, the channel effects are introduced to the data in the bandpass. The realization of different delays for a certain tap is not is not as flexible as in the software case. As mentioned previously, a PDP is assumed to be constant within a local area. It changes from one local area to another where the number of taps and their delays may change. Therefore, the hardware channel emulation is for a predefined channel scenario. However, the Doppler spectrum can still be introduced to the signal that leads to the variations in the amplitude values of the channel taps.

3.4 Chapter Conclusion

This chapter presented the survey performed by the authors for some software channel models and hardware based channel emulators. Different means of introducing the delayed taps and Doppler shift were presented. The strengths and the weaknesses of applying the channel effects to the signal in software and hardware were also studied. The next chapter contains a software-based channel model proposed by the authors that works for the FM band in an outdoor environment. To the authors best knowledge, it is the first model that serves this band. Thereafter, a hardware based channel emulator will be introduced.

Chapter 4

Software-Based FM Wireless Channel Model

The previous chapter gave a quick overview on some software channel models and hardware emulation techniques. Proposed in this chapter is a software FM model[1] that is based on the COST 259 model slightly explained in the previous chapter [10, 12]. The COST 259 model works for a wide range of frequencies and for the four distinct types of outdoor environments mentioned in the previous chapter. However, the FM band is not supported by the COST 259 model.

4.1 Background of the Approach

The attention of the authors has been drawn to the precious FM Band that is considered to be very poorly utilized by an analog radio broadcasting almost all over the world. This poor utilization arises from the fact that most people have now switched to the Internet streaming of voice media instead of the traditional FM radio channels. The decreasing number of users listening to FM radios and the inefficient analog transmission of the band are now calling for the deployment of more efficient wireless systems. As the FM Band occupies a portion of the VHF band with $\approx$ 20 MHz bandwidth, it has good propagation characteristics that can provide large coverage distances. This connotes an

---

[1]This software FM channel model has been accepted by the Canadian Journal of Electrical and Computer Engineering (CJECE) with the name "A Directional FM Channel Model for Contemporary Wireless Systems"

ideal scenario for switching to a more efficient digital transmission from a voice only analog system. Indeed, a similar scenario had existed for the TV broadcasting systems in some countries including the USA. There, the analog TV band around 700 MHz was enjoying the broadcasting luxury for analog TV channels but then the band was chopped for digital services, public safety systems, and cellular operations targeting the rural areas. As for the FM Band, a cellular mobile system that rely on multiple antenna techniques and that provide public safety services can be developed since there is a large enough bandwidth to support acceptable data rates. For the deployment of a digital communication system in the FM Band, the wireless channel properties should be known well ahead for accurate performance analysis. The literature, in general, lacks channel modelling for the FM band. We have performed an extensive literature survey for the studies dealing with the FM channel modeling relying on the measurements but unlike other frequency bands, the amount of studies for this band is very minimal as the analog transmission of the FM Band is taken as granted. Therefore, the survey included the studies performed for the bands nearby the FM Band.

The COST 231 model and its extension in [35] are suitable for bands from 150 MHz up to 2 GHz, and hence are not directly usable for the FM Band. Similarly, the study given in [13] presents parametrization and validation of the COST 2100 channel model for peer-to-peer communication in the 300 MHz band. As shown in Table I of [12], the COST 259 model was developed for the range of 150 MHz - 2 GHz for HTRs, but it was parametrized for the frequencies between 500 MHz - 2 GHz. Hence, this model is not directly usable for the FM Band as well. The work in [36] proposed a path loss model for 110.6 MHz but it lacks the key aspects of wireless channels such as the directionality and the multi-path profile. Clearly, the model is incomplete to be used for contemporary wireless systems. Similarly, measurements of a HTR channel at 145 MHz targeted the development of a multi-path channel model that is suitable for single antenna transceivers [19], [6]. A power level measurement study seeking a model for determining the path loss was found in [37], and obviously the model lacks many of the key parameters of a contemporary channel model. Thus, it is clear that no complete channel model has yet been proposed for the FM Band.

When developing channel models, usually certain measurements are performed to extract typical channel parameters. The reported FM Band measurements in the literature however, are mostly for power levels and do not bear full information for a directional channel

modeling with delay information. Due to the lack of suitable measurements for this band, the proposed model made some informed assumptions about channel modeling parameters. Our assumptions and recommendations are explained by the understanding of the physical channel and for some cases they have been validated via Wireless Insite simulations, a commercially available RF ray tracing tool. We understand that extensive measurements should have been carried out in order to validate the assumptions. However due to the FM Band regulations and full occupancy of the band, the measurements are left for a future task . Here, our approach is to model the FM channel for HTRs by exploiting the raw data measurements performed for the same type of environments in a nearby frequency band, which is 145 MHz [19] and [6]. This can provide a close scenario for comparisons with the developed model and simulations via Wireless Insite Suit.

The statistical model proposed in this study can be considered to be an extension to the COST 259 model [10, 12], with some deviations stemming from the measurements available for the nearby frequency bands and the understanding of the physical channel behavior for the FM Band. The COST 259 model basically has many parameters in deriving the PDP and then extracting the CIR. The modelling of these parameters were proposed to adapt to the 2 GHz band. Clearly, these modeling methodologies of the channel parameters need to be modified so as to fit the FM band. A separate section will be introduced that has many subsections, each of which is dedicated for a certain parameter model. The deviation from the existing model and the newly proposed model will be presented. Another Section will clarify how to get the PDP for the FM Band from which the CIR can be drawn. The choice of the COST 259 model as a foundation for this study was due to many reasons but it being one of the latest proposed statistical channel models is the key advantage. It is also considered to be relatively simple, general, and appropriate for a wide range of environments. The inclusion of the third dimension in the modeling also plays a critical role. Many of the past channel models did not take this dimension into account. Its importance becomes clear when MIMO systems are required to take the advantage of the arrival of different multipaths from different directions as mentioned earlier.

As in the case of [12], the proposed model adopts the concept of circular clusters visibility regions within which the receiver can receive a certain cluster that might be coming from the Base Station directly in the LOS case or from an IO in the NLOS case.

4.2 Parameters

4.2.1 Number of clusters

The model presented in [12] followed the assumption of the existence of at least one cluster anywhere in the operation region. In [13], two types of clusters are identified: far clusters and local clusters that were observed almost everywhere the measurements were taken. Based on these earlier studies, the model presented here will follow the same assumption of the existence of the local clusters. Therefore, the first cluster of the model can be LOS or NLOS, while the existence of the rest of the clusters is determined according to the presence of the receiver in the visibility region of the corresponding cluster. Note that the criteria on which the first cluster will be decided to be an LOS cluster or NLOS one is also the visibility region criteria. If the receiver does not lie inside an LOS visibility region, then the local cluster that always exist is an NLOS cluster.

The visibility regions of the clusters, excluding the local one, will be assumed to be circular with the same radii lengths as proposed in Table III of [12]. Depicted in Fig. 4.1 is the illustration of the assumed circular visibility region of such a cluster due to an IO. This approach will also simplify the implementation of the model in simulation environments.
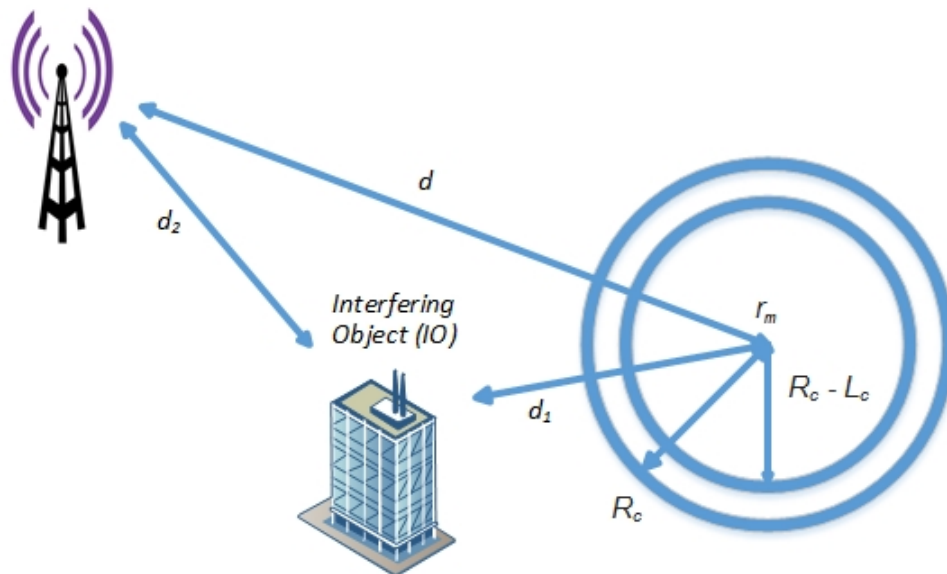

FIGURE 4.1: Illustrative figure for the circular visibility regions.

As a first step, the whole operation area is divided into circular visibility regions using the hexagonal packing of circles that gives the maximum density of covered area. This

guarantees that most of the operation region is covered by the circular visibility areas. The number of clusters, excluding the first, for each of those circles is then taken as a Poisson random variable with a decreasing mean as the planar distance d from the transmitter increases. This is in contrast with [12] that just assumes a constant mean of the number of non-first clusters (the clusters excluding the first) per circle among the whole operation region. This can be interpreted physically as follows: as the distance from the transmitter increases, the probability of the signal's survival decreases, causing the large-delay clusters to die away before reaching the receiver. Therefore, clusters become barely received by the receiver as the distance from the transmitter increases. The available 145 MHz measurements performed for HTRs were carried out at a set of locations with different distances from the base station (BS) [19], [6]. At each of those locations two measurements were taken: one measurement while going away and another one while coming back to the BS. According to these measurements, the mean of the Poisson random variable at the center of each of those circles can be modeled as:

$$\lambda = max\left\{ \left(\lambda_i' - (0.2726 * d) \right) - 1, 0 \right\}. \tag{4.1}$$

Here, λ_i' is the initial average total number of clusters at zero distance from the transmitter and d is in kilometers, while the subtraction of 1 in the formula is to account for the always assumed existing first cluster. This linear formula was found to be a good fitting, as will be discussed in the validation section. However, it should be noted that the expression in (4.1) may change dramatically when the wireless region is not of HTR type. In such scenarios, the number of clusters may even increase in some extreme cases. The modeling of the mean as a decreasing quantity as the distance between the transmitter and the receiver increases is considered to be the most general and convincing scenario. This assumption of decreasing number of clusters agrees with the 145 MHz given measurements [19] and [6] as well as the simulations. For our case $\lambda_i' = 3.5$ was found to be a suitable value for the linear fitting of the straight line with the available data. The reason for choosing such formula with those suggested parameters values will be discussed in the validation part in more details.

The LOS circular visibility regions ought not to be confused with the non-first clusters visibility regions since they are generated separately with the same suggested radii values proposed in Table IV of [12]. The LOS circular visibility regions are generated with the

hexagonal packing of circles too, but what determines the existence of LOS within each circle is a Binomial random variable with the probability of being LOS circle given as:

$$p_{LOS}(d) = max\left\{\frac{d_{co} - d}{d_{co}}, 0\right\} \qquad (4.2)$$

where d_{co} is the cut-off distance after which no LOS is observed and d is the planar distance between the center of each of those circles and the transmitter. According to the given 145 MHz measurements [19], [6], d_{co} is suitable to be equal to 1000 meter.

4.2.2 IO location

For simplicity, only one IO will be assumed to trigger all the non-first clusters as in the case of [12]. If more IOs are to be taken into consideration then the implementation would be more complicated contributing into a marginal accuracy. The typical delay spread values for HTR at different frequencies of operation can be checked from Table 3.1. Plotting all these points and by coarsely fitting them, it can be found that the expected typical values for the delay spread at the FM Band is close to 40 μsec at distances close to the transmitter. This increase in the delay spread as the frequency decreases in the outdoor environment can be related to the propagation characteristics. For a given distance, the propagation loss decreases as the frequency decreases, which in turn increases the probability for the waves to travel to further IOs and be received by the receiver without vanishing. The relation between the distance from the transmitter, the cluster delay spread, and the overall delay spread will be discussed in details in the next subsection.

The approach for IO location modeling of this study is a deviation from the existing art in [12]. The COST 259 model modelled all the IO locations of a certain circular visibility region by drawing their coordinates from a two-dimensional Gaussian distribution centered on the corresponding visibility region center r_m as shown in Fig. 4.1. The problem with this method is that it leads on average to the overlapping of clusters in time in most of the cases, so the extra arriving clusters do not contribute in the increment of the total delay spread to a great extent. However, this is not the typical actual case where clusters arrive generally at different times with a certain probability of overlapping in time. Therefore, the approach taken by [12] for the modeling of the IOs locations is not

very suitable for the FM Band. Besides, with the modeling of IO locations proposed in [12], getting the expected amount of the delay spread of the FM Band will be a very rare case. Hence, we adopt an alternative approach for the modelling of the IO locations so that typical delay spreads of the FM Band are realized.

To overcome this issue in the present model, the arrival time of the first cluster is estimated by considering the distance between the transmitter and the center of the corresponding circle to which the non-first clusters belong. Then the arrival time of each of the following cluster is assumed to happen after that of the preceding cluster and to be distributed by an exponential random variable. Hence, we can obtain the arrival times of all of the non-first clusters. A mean of about 10 μsec was found to be well-suiting the given 145 MHz measurements [19], [6]. The total distance travelled by the cluster between the transmitter and the receiver is then divided into d_1 and d_2 as shown in Fig. 4.1. Once the IO location is determined, the corresponding cluster's features are determined via simple geometry. The suggested approach was found to be more efficient to get the expected total delay spreads. Thus, with the modeling proposed in this study, the non-first clusters features are modeled differently but similar to the famous Saleh and Valenzuela model in [11]. As for the first cluster, its features are obtained exactly as proposed in [12]. Therefore, our proposed model can be considered as a hybrid approach.

4.2.3 Clusters Spreads and Shadow Fading

Here, a similar approach given in [12] is followed, but different values for the parameters so as to adopt them to the FM Band are introduced. The standard deviation of the log-normally distributed shadow fading in dB scale is given by 6 dB for 2 GHz, while in the 145 MHz measurements in [19] and [6], the standard deviation is given by 6.25 dB. Hence, it is apparent that the log-normal shadow fading random variable is not too dependant on frequency of operation as long as there is no change in the environment type, which is HTR in those studies. Therefore, it is expected that the standard deviation of the shadow fading random variable for the FM Band will not be far away from 6 dB.

For the delay spread, it was clearly stated in [38] that the median delay spread increases as the distance from the transmitter increases. This is very acceptable in the outdoor environments for the high frequencies of operation where only one cluster is received by the receiver in most of the cases according to Table II in [12]. Receiving only one

cluster indicates that the delay spread of the cluster is the same as total delay spread of the channel. Therefore, the total channel delay spread increases as the distance from the transmitter increases. However, as discussed earlier, for the case of low frequency of operation, the number of clusters decreases on average as the distance from the transmitter increases, and the number of received clusters is generally greater than one in the vicinity of the transmitter. The total channel delay spread is not the same as the cluster delay spread in case more than one cluster exists. Therefore, the average increase in the cluster delay spread as the distance for the transmitter increases does not have to imply a corresponding increase in the total channel delay spread. In fact, it is the opposite of that for the given measurements at 145 MHz [6]. This means that the arrival of extra clusters at relatively small distances from the transmitter compensates the increment in the delay spread of the cluster as the distance from the transmitter increases. This is because the clusters mostly arrive separately in time. To sum it up all, according to the given measurements in [6], the cluster delay spread increases as the distance from the transmitter increases but the total channel delay spread decreases because the extra time taken by the following clusters to arrive is typically larger than the increase in the cluster delay spread due to the increase of the distance from the transmitter. Therefore in the modelling, the same cluster delay spread formula presented in [12] is used here but with a median cluster delay spread for 1000 meter separation between the transmitter and the receiver of 5 μsec according to the given measurements in [6].

The measurements performed at 145 MHz do not provide any information concerning the angular spreads [19], [6]. To get the required parameters for the modelling of the angular spreads, a review of the available angular measurements performed at different frequencies of operation is required. As reported in Table IX in [12], the suggested median of the log-normally distributed azimuth angular spread for the *urban* areas was 10° with a standard deviation of 3 dB. This means that the mean is approximately 10.2^o. This was validated at 2 GHz [12]. In [13], the study of the angular spread at 300 MHz was on two basis: whether it is an LOS case or not, and whether the angular spread is at the transmitter or the receiver. However, according to the given values, there seems not to be a significant difference between the transmitter and the receiver case, although the angular spread at the receiver is greater. On the other side, there is a considerable difference in the means of the angular spread between the LOS case and the NLOS case. Among all the different cases, the lowest given mean was 14.6^o, which is

much larger than the value reported in [12]. According to this, it is clear that there is an inverse proportionality between the frequency of operation and the angular spread. By averaging the LOS and the NLOS case, it is expected that the median angular spread for the 300 MHz band in HTR will be around 8°. It is also expected to increase even more for the FM Band case. Thus, the same suggested formula in [12] is used in this study with a median angular azimuth spread at the BS of 9°. For the rest of the angular spread values, the same expressions in [12] are used with the same parameters.

Regardless of the increase in the cluster's angular spread, the relatively high number of received clusters in the vicinity of the transmitter increases the overall channel angular spread. Therefore, the total channel angular spread is expected to increase in the FM Band case compared to the higher frequency bands.

4.2.4 Clusters Gains

The power gain equations in [12] are used with different parameter values. The k_τ factor, that represents the increase in the decay of the power of the non-first clusters with their delay, was more appropriate to be equal to 2 dB/μsec according to the 145 MHz measurements [6]. Also τ_B that represents the maximum non-first cluster latency after which there will be no more average power decay in order not to make that cluster vanish completely is given by 15 μsec.

Moreover, the correction parameter $s(d)$ has also been changed to accommodate the current model. $s(d)$ values were set for different distances d from the transmitter in order to generate the expected received power levels in the FM Band. The use of the correction parameter was initially proposed in [39], where $s(d)$ values were determined by Monte Carlo simulations. Based on the 145 MHz measurements [6], the received power levels for the 100 MHz were estimated. Monte Carlo simulations for each of the distances d from the transmitter presented in Table 4.1 were performed iteratively. The chosen stopping criteria for each single point measurement was yielding an average received power level that is within a 2 dB range from the expected received power level in the FM Band. Presented $s(d)$ values in Table 4.1 are those used in the last Monte Carlo simulation for each of those distances. The correction parameter $s(d)$ usage in the model can be found in equation (11) in [12].

TABLE 4.1: Correction parameter values for different distances from the transmitter

d	$s(d)$
0.508444	17E+13
0.902649	470E+08
1.422356	1.5E+09
1.517287	5E+10
2.347531	4.5E+09
2.725646	1.6E+10
2.955733	2.3E+10
3.032965	2.2E+10
3.390163	2.1E+10
3.444869	1.6E+10
3.549454	5E+11
3.898607	4E+11
4.439231	2E+11
4.849526	1.5E+11
5.329008	5E+09
5.789182	4E+09
6.101328	1.45E+10
6.534149	1.3E+10
6.968579	2.4E+10
7.460933	4.5E+10
7.938806	5.8E+09
8.410243	4.5E+10
8.933168	5.8E+09
9.388515	1.7E+10
9.837426	2.3E+10
10.56952	5E+10
10.91063	7E+09
11.28874	2.7E+10
11.50757	1.2E+10
11.8165	3.7E+10
12.37643	2E+10
12.83982	3.9E+10

P_{NLOS} in the power gain equations in [12] represents the NLOS path gain, but it cannot be derived from the COST 231-Hata model for the rural and hilly environments because the COST 231-Hata model does not work for the FM Band. Fortunately, a study for the path loss for the FM Band was found in the literature [37]. Hence, P_{NLOS} value is derived from the formula proposed in [37] using the suburban area formula that is expressed as:

$$L = L_b - (2 * ((log(f_c/28))^2)) + 7.46 \qquad (4.3)$$

where f_c is the frequency of operation, L_b is derived from equation (4.4.3) in [35] using the suburban area formula and L is the actual path loss in dB that is to be converted into linear scale and then P_{NLOS} becomes its reciprocal (gain).

4.3 PDP & CIR

The number of MPCs within a cluster are determined according to the time resolution of the receiver as assumed in [12] in order to result into a Rayleigh fading for each resolution bin except for the first bin of the first cluster if LOS exists, which then has a Ricean fading. The resolvable delay bin time was assumed to be 0.2μsec in [12] since the maximum bandwidth B of the receiver is 5 MHz and the bin-width is given by $1/B$.

In the current model, the cluster delay spread is usually much greater than the resolution delay bin since the median cluster delay spread at 1 km distance between the transmitter and the receiver is about 5 μsec. Dividing each cluster delay spread by the bin-width results in a number of bins within each cluster. Each of those bins will be modelled to contain 15 MPCs, which then form a Multi-Path Group (MPG) as discussed in [12]. According to [12], 15 MPCs per bin is a large enough number of MPCs to result into a Rayleigh distributed amplitude bin. MPG is a group of MPCs that are unresolvable by the receiver because they are approximately identical in their DOA and arrival time (same bin), and hence a cluster contains at least one MPG.

The uniform distribution of the arrival time of each MPC within the delay bin it belongs to will result into the desired bins amplitudes distributions according to [12]. The main MPC in each cluster is characterized by the same arrival time, departure angle, and arrival angle as those of the cluster itself. Therefore, there is no randomness in determining the features of the main MPC of the cluster once the features of the local or the far clusters are detected. For the rest of the MPCs within the same cluster, their angles are generated uniformly over the interval $[(\theta - \sigma_\theta/2) \ (\theta + \sigma_\theta/2)]$. Here, θ is the cluster's azimuth/elevation angle computed after determining the cluster's features geometrically as described previously, while σ_θ is the angular spread computed according to the explanation in the last section.

After being able to determine the MPCs arrival times and angles, the relative power delay/directional profiles are computed by exploiting equations (16-21) given in [12].

These equations connote the decrease in the relative power of a certain cluster's MPC with the increase of its delay/angular separation from the cluster's main MPC.

Within each delay resolution bin, all the MPCs' powers are summed together to give a certain resolvable MPG at the receiver. The relative power of each MPG is then multiplied by the previously calculated corresponding cluster path gain. The outcome of this is then multiplied by the transmitted power to give the actual received power level. The antenna gains were not taken into consideration in the equation below for the sake of simplicity and generality of the model. However, if the antenna gains are determined they should be then multiplied by the path gain to get the total received power.

The relative PDP per each delay bin is then given by

$$P_{relative} = \left(\sum_{i=1}^{K} P_{MPC_i} \right) * P_m \tag{4.4}$$

where K represents the number of MPCs within the single delay bin, which is considered to be 15, P_{MPC_i} is the relative power of the ith MPC in the delay bin, and P_m refers to the path gain of the corresponding m^{th} cluster to which the MPC belongs.

Note that different clusters may overlap in time, and in this case the relative powers of the overlapping delay bins are summed up together to give a certain pulse at that time instance, although they might be received from different arrival angles.

To generate the CIR from the PDP within each bin, the amplitude of the response for each bin is taken as a Rayleigh random variable of scale parameter σ where σ^2 is equal to the value of the power of that delay bin. This is due to the fact that σ^2 represents the time-average power of the received signal according to [16].

As for the LOS case, the same approach of the COST 259 model applies. The Ricean factor is firstly modelled as described in section IV.F in [12] and then equation (23) in [12] is taken into consideration for calculating the relative MPCs powers. The contribution made here was adjusting the correction parameter values so that the simulations and the expected received power levels match as mentioned in the previous section.

4.4 Validation

A MATLAB code that implements the channel model for the described framework has been developed. A large number of channel realizations have been generated to check how close the results will be to the expected PDP and to the measurements in [19] and [6]. Presented in Fig. 4.2 is one of those realizations representing the relative PDP, which is multiplied with the power gains of the clusters at a distance of about 5 km from the transmitter.
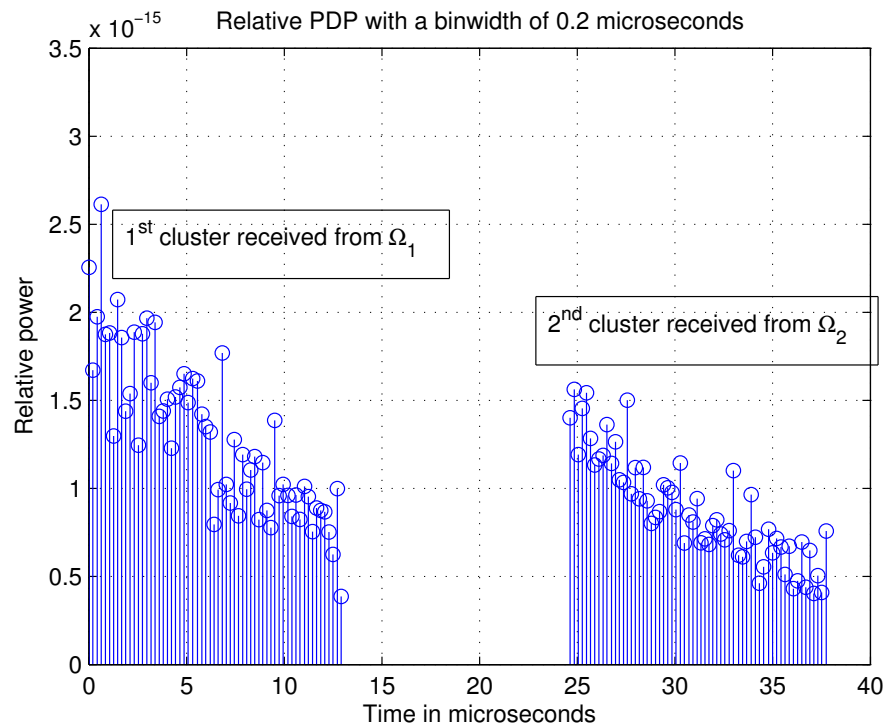

FIGURE 4.2: Relative PDP where Ω_i represents the Angle of Arrival of the ith cluster.

After investigating different PDPs that resulted from actual measurements, it was found that usually there is no such sharp drop in the power level that appears between the two clusters in the presented relative PDP realization in Fig. 4.2. One of the possible physical interpretations of this issue is the presence of noise in the actual measurements that does not make the power jump directly and stay in the zero level till the arrival of the following cluster.

4.4.1 Number of clusters

The graph shown in Fig. 4.3 is based on the limited available 145 MHz measurements in [6]. It shows how close the proposed linear formula of the number of clusters to the actual measurements performed in [6]. As mentioned earlier, it is assumed in the model that at least one cluster exists. Hence, the mean of the Poisson random variable, representing the number of *extra* clusters at the center of each circle, is taken to be the straight line depicted in Fig. 4.3, except that it is decreased by one to discount the always existing first cluster. According to the given 145 MHz measurements [6], this assumption does not seem to be an invalid hypothesis among the whole operation region, which is about 13 kilometers from the transmitter.
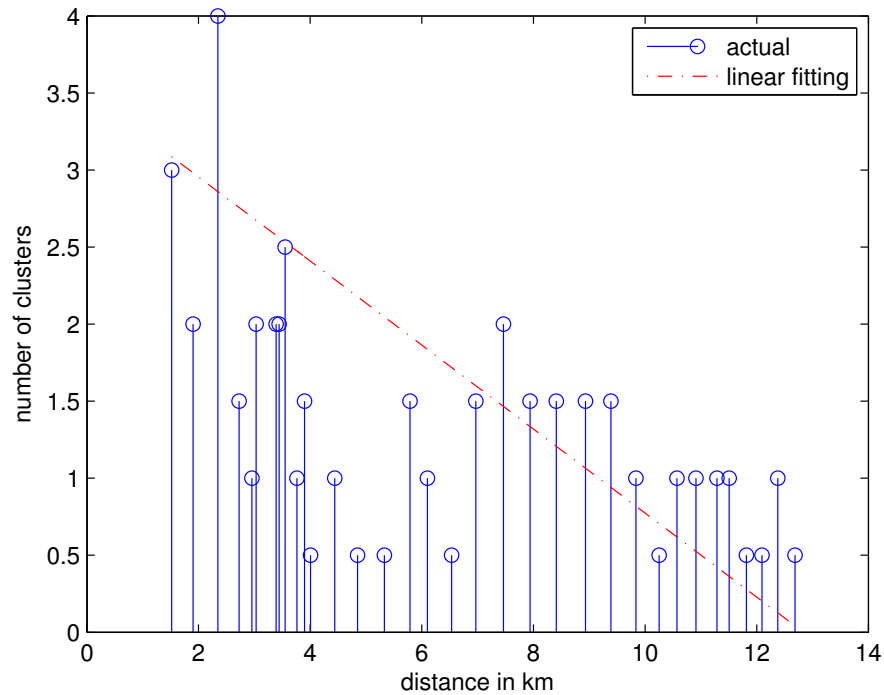

FIGURE 4.3: Comparing figure between the actual measured average number of clusters at 145 MHz, [6], and the proposed linear formula vs. the distance from the BS.

Although 145 MHz measurements, [6], are not for the desired band, we do not expect the measurement results to be very much deviating from the FM case since it is very close to the FM Band. Besides, those measurements were the closest measurements to the FM Band found in the literature when the channel parameters of this study are concerned. In the measurements, no clusters were observed at all after a distance of about 13 kilometers from the transmitter, and therefore the linear formula was assumed

to be zero there. While at closer distances of about 7 kilometers from the transmitter, two clusters were observed once and one cluster was observed at another time, an average number of clusters of 1.5 was assumed there. Assuming a straight line equation for simplicity, the equation of the straight line is plotted in Fig. 4.3. For zero planar distance from the transmitter, the value of the mean number of clusters was also chosen according to Fig. 4.3 as λ_i'=3.5. If the straight line is extended to zero it will almost intersect the y-axis at 3.5. Hence, according to the comparative Fig. 4.3, the proposed linear formula with the suggested λ_i' value seems to be a good proposal.

If the number of clusters is determined according to their relative powers not according to the absolute power of the received cluster itself, then this formula might not work. This is due to the fact that in the vicinity of the transmitter, there is a high chance of receiving LOS component, which has a very high power compared to the rest of the clusters. The high power cluster then becomes the only visible component to the receiver. This is why relatively far locations from the transmitter were chosen to derive the linear formula where almost no LOS is observed.

4.4.2 Total delay spread

RF ray tracing simulations were performed by the authors to check the validity of the claim that the total channel delay spread may decrease as the distance from the BS increases. Fig. 4.4 shows a three dimensional view of the simulated hilly environment, which was chosen to be in Konya, Turkey. On the other hand, Fig. 4.5 depicts the project elevation view with the place of the transmitter and the sets of receiver locations. An isotropic transmitter with an input power of 45 dBm was placed above all the receivers with a center frequency of 100 MHz and a bandwidth of 5 MHz. The receivers sensitivity were set to −120 dBm. The receivers were divided into different sets, where each set is characterized by a constant planar distance from the transmitter. It was desired to deal with the worst case (largest delay spread), and therefore each set was represented by the receiver having the maximum delay spread within this set. The sets were then arranged according to their maximum delay spread and via simulations it was found that at distances above 6.5 km, the maximum delay spread of each set decreases as the distance of the set from the transmitter increases.
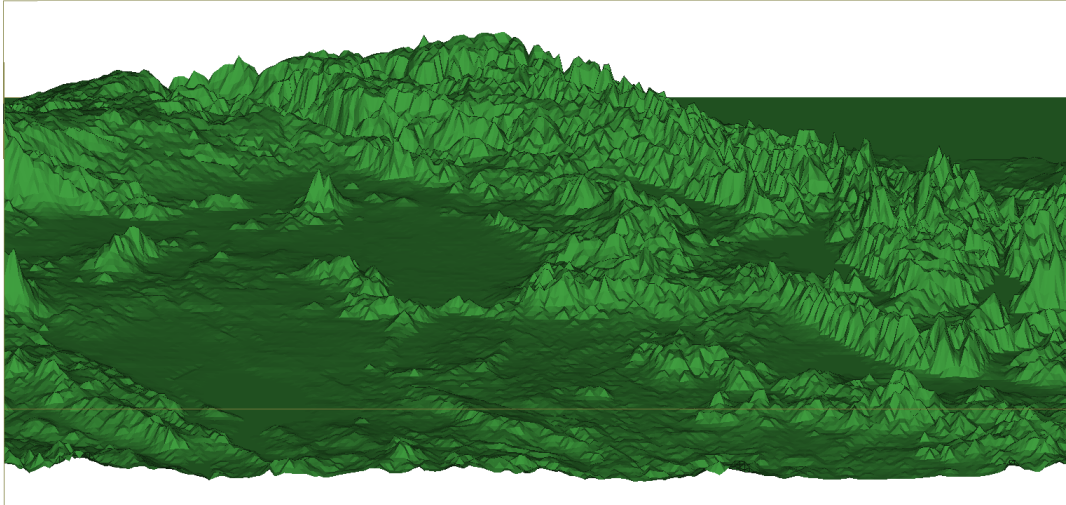
FIGURE 4.4: Three dimensional view of the simulated environment in Konya, Turkey.
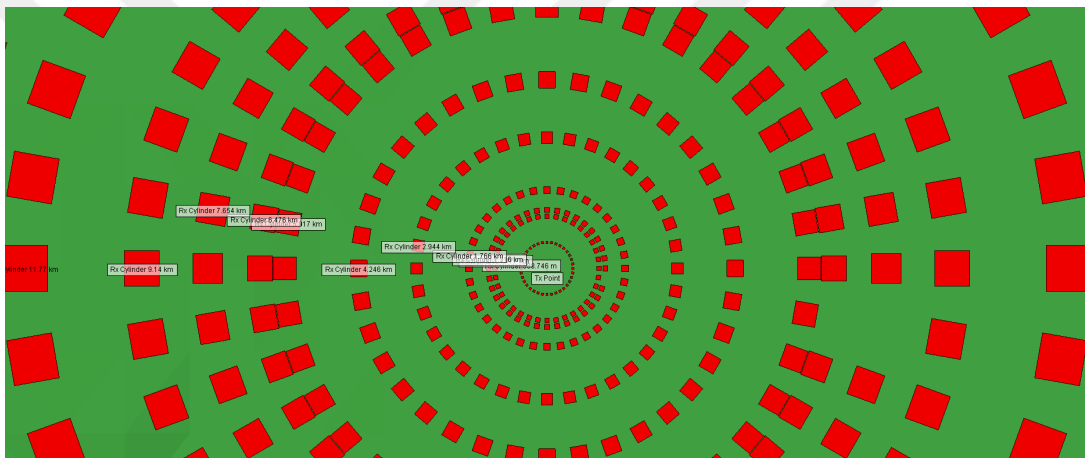

FIGURE 4.5: Project view of performed Wireless Insite simulation in Konya, Turkey. Isotropic transmitter is placed in the center and receivers were placed as cylinders around the transmitter.

For distances below 6.5 km, the simulation results were opposite of the earlier case. The physical interpretation for this is that at small distances there is a high chance of receiving LOS from the transmitter, which has very large power compared to the power of the rest of the clusters. This reduces the overall delay spread. This still does not mean that the receiver did not receive other clusters. However this effect will be more apparent in the maximum excess delay rather than the root-mean-square (rms) delay spread. This is because the maximum excess delay does not deal with the relative powers of different MPCs as long as the power of each of them is larger than the receiver sensitivity value. Moreover, that decrease in the total delay spread as the distance from the transmitter increases supports our proposal concerning the decrease in the number of clusters.

4.5 Chapter Conclusion

With the availability of more extended measurements, this model can be taken as a basis for new sub-models in order to better fit the FM Band. It is observed that one of the characteristics of the FM Band channels is the increase of the angular spread due to the increasing number of clusters. Hence, systems based on MIMO antenna technique can be deployed in the FM Band with high performance, resulting in a higher bits per hertz systems. Another key observation is the presence of very large delay spreads in the FM Band. For the deployment of systems based on orthogonal frequency division multiplexing (OFDM), this implies a very large Cyclic Prefix (CP). This leads to a very long symbol duration, which in turn means low data rate. Therefore, the utilization of generalized frequency division multiplexing (GFDM) considered for 5G systems might outperform OFDM systems since it can overcome the problem of the channel coherence bandwidth being smaller than the bandwidth of each sub-carrier [40].

Next chapter includes the implementation of a hardware channel emulation technique. The channel effects are introduced to the signal in the RF domain without the need to process the signal in the baseband after its downconversion.

Chapter 5

Hardware implementation

Typically, the received signal is the processed version of the transmitted signal. This processing is done by the channel where time and frequency dispersion are being introduced to the signal. Noise is then added to the smeared version of the signal. This noise is widely accepted to be modelled as Additive White Gaussian (AWG) that has a flat power spectrum over all frequency contents and whose distribution is Gaussian with zero mean. The addition of the noise to the smeared signal is a simple task where there is plenty of AWG noise (AWGN) generators that can be utilized. This chapter will show the proposed method to introduce the channel effects -namely time distortion and Doppler effect- onto the signal in the bandpass.

5.1   Channel delay taps

It was mentioned earlier that the approach of introducing delay to the channel taps by means of cables extension turned out to be impractical especially when a large delay is required. According to Table 3.1, it is clear that low frequencies of operation in the outdoor environments are accompanied with large delay spread values. Therefore, to emulate a wireless channel operating in a low frequency, the cables approach becomes non-feasible due to the bulkiness of the hardware emulator. The choice was to emulate a predefined outdoor channel operating at 140 MHz that is typically characterized by large delay spread values.

A surface acoustic wave (SAW) is a type of mechanical wave motion traveling along the surface of a solid material. The wave was discovered in 1885 by Lord Rayleigh. A basic SAW device consists of two interdigital transducers (IDTs) on a piezoelectric substrate such as quartz as shown in Fig. 5.1 [7]. In a SAW filter, the electrical signal is converted to an acoustic wave and then back to an electrical signal. Large delays are easily acquired making use of the advantage that acoustic waves travel very slowly (typically 3000 m/s). The IDT geometry is capable of almost endless variation, leading to a wide variety of devices. Starting around 1970, SAW devices were developed for oscillators, and bandpass filters for domestic TV and professional radio. In the 1980s the rise of mobile radio, particularly for cellular telephones, caused a dramatic increase in demand for filters. New high-performance SAW filters are produced in large numbers.
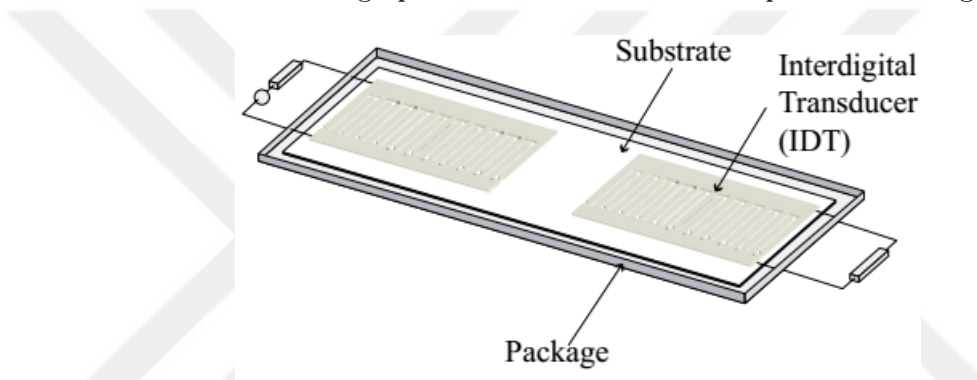

FIGURE 5.1: Basic SAW Device [7].

The idea of utilizing SAW filter was adopted in [34]. According to the previous explanation, SAW devices can be designed to introduce large group delays that can be exploited to generate large multipath delays in laboratory environments. Note that most of the commercially available SAW filters are bandpass filters with different center frequencies.

Therefore, for the case of large multipath channel delay taps being required, the use of SAW filters is preferred to the use of cables because they would be much smaller in size and cheaper than the bulky elongated cables. Moreover, many of the SAW filters manufacturers offer the luxury of ordering a customized SAW filter that gives the desired group delay values. This is in addition to the availability of a large variety of SAW filters offering different group delay values at the desired bandpass. Note that their phase response is almost linear. This results into very small tolerance in the specified group delay along the whole passband.

In [34], two emulation techniques were described: The Cascade Connection Technique and the Feedback Technique. The cascade technique is simple where SAW filters operating at the same center frequency are being cascaded to offer a larger delay for the tap if required. The amplitude and the phase of the tap can be controlled via attenuator/amplifier and phase shifter respectively. Another choice is to replace the cascaded small-delay SAW filters with another one that operates at the same center frequency but offers a higher group delay. This solution is feasible due to the availability of a wide range of SAW filters at a certain frequency as mentioned before. The cascading technique is shown in Fig. 5.2.
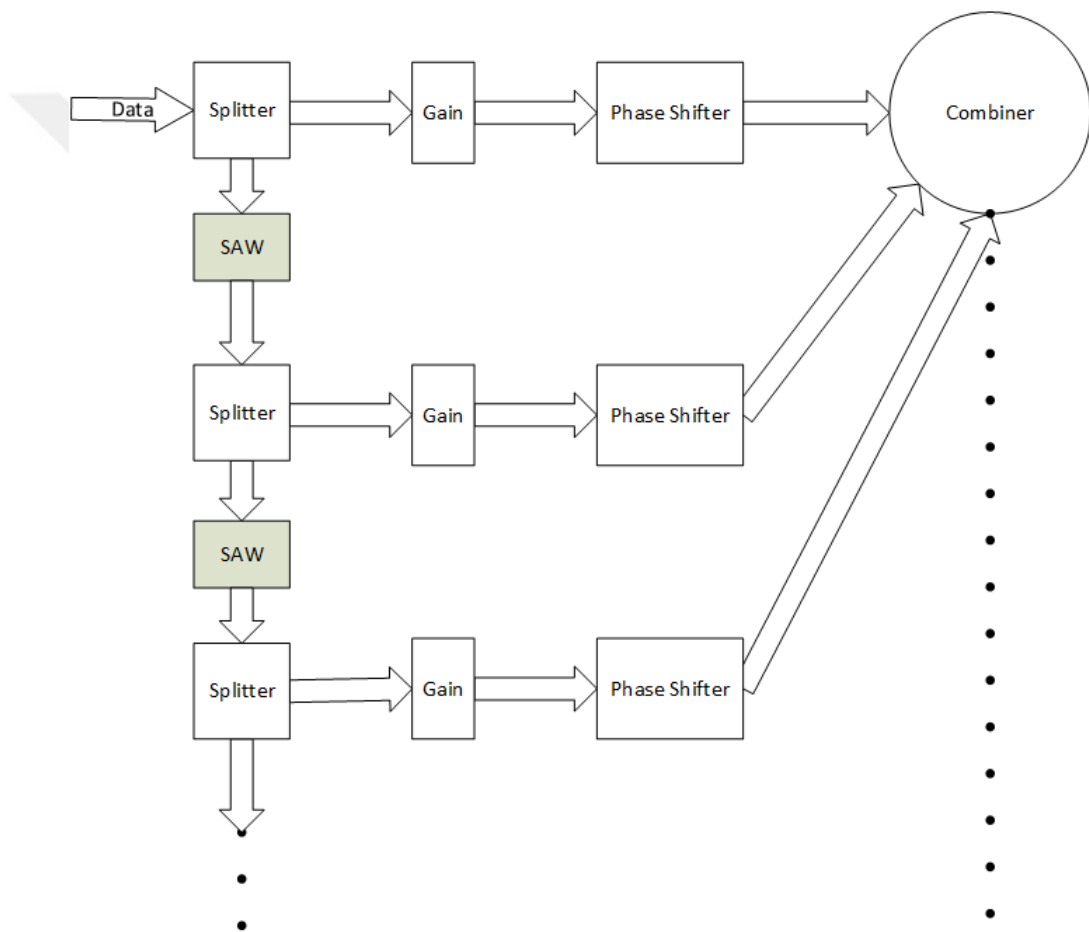

FIGURE 5.2: Cascading technique of SAW filters

The feedback technique basically depends on entering the output of the first tap to the SAW filter once again in order to result into other taps that are equally spaced in time domain with the same group delay amount the SAW filter offers. The amplitude and the phase of the first tap is fully controllable through the attenuator/amplifier and the phase

shifter respectively. As for the rest of the taps resulting from the loop, there is no control over their amplitudes and phases since they depend basically on the first entering data sample. However, the generic shape of the resulting taps amplitudes can be controlled via gain blocks (attenuators/amplifiers) where an exponentially decaying power response might result. Note that the SAW filter itself also has its own insertion loss, which is also in scale of dB. Thus, the resulting PDP is typically an exponential decay even when no attenuators/amplifiers are used. The number of the resulting taps from the loop can also be controlled through a variable attenuator that can play a role in determining the maximum excess delay. The feedback technique is shown in Fig. 5.3.
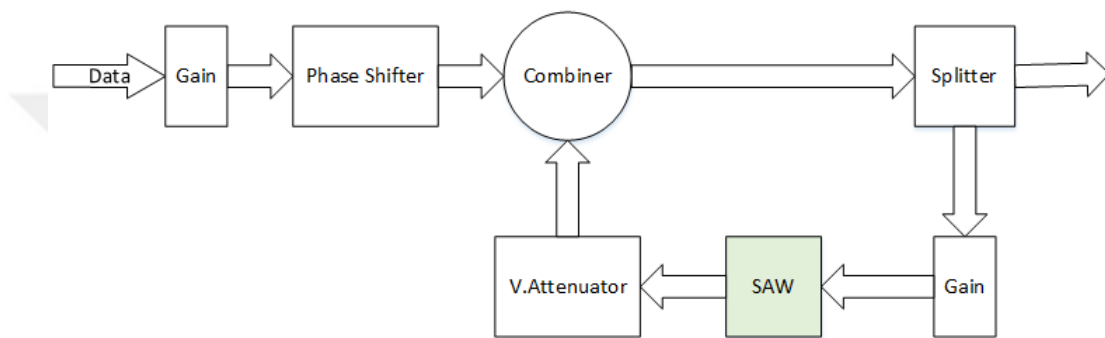

FIGURE 5.3: Feedback technique

The cascaded technique is helpful when the predefined channel has relatively low number of channel taps. In such a case the cascaded technique would be more efficient than the feedback technique due to the presence of full control over the amplitudes and phases of the taps, in addition to the possibility of getting unequally spaced taps in time if it is desired. However, in many cases especially when the total channel delay spread is large, the number of desired channel taps to be emulated is large and hence, it might be impractical and very expensive to assign each of those taps a dedicated branch as shown in Fig. 5.2. In that case, it may be a possible solution to utilize the feedback technique in emulating clusters. As mentioned before in Chapter 2, the PDP within each cluster generally decays exponentially with time. Therefore, the feedback technique can be used to emulate a single cluster where the first tap of the cluster is fully controlled while the others are not. Thus, the proposed emulation method when there is more than one cluster with large number of taps required per cluster is the combination of both of the techniques with each branch resulting into one cluster whose PDP decays exponentially with time. Each cluster is assigned to a branch where the maximum excess delay of the cluster can be controlled via the variable attenuator of the corresponding branch.

Note that at low frequencies, there is typically more than one cluster in the outdoor environment. Fig. 5.4 shows the proposed emulation hybrid technique. There, the SAW filters on the left side of the figure are for determining the cluster's first tap delay while the SAW filters in the loops are for determining the time delay between each two successive taps within the same cluster.
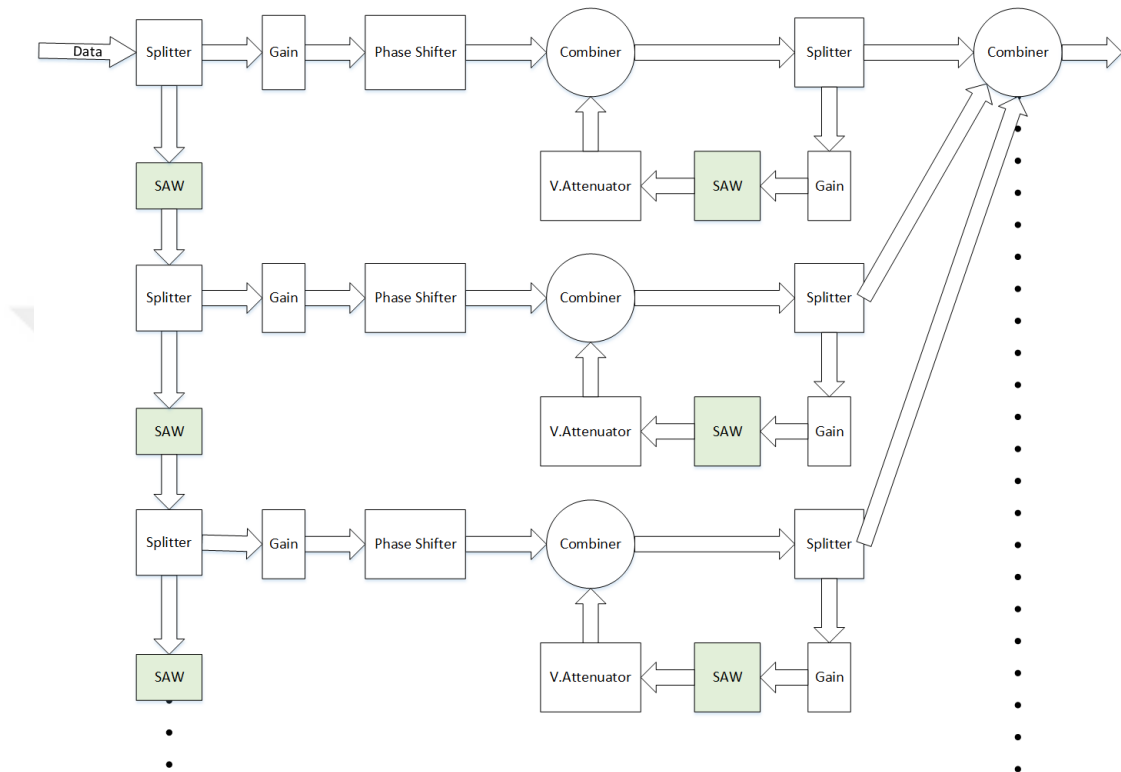

FIGURE 5.4: Hybrid technique with each branch corresponding to a cluster whose maximum excess delay can be controlled via the variable attenuator of that branch

Though its inability in controlling all the clusters taps, this method is still considered to be cost efficient when outdoor low frequency channels are desired to be emulated with a very large number of taps per cluster required. It is worth to remind that the number of required taps in the channel delay spread depends on the symbol duration of the utilized communication systems. For instance, the transmitted symbol duration in the modern OFDM systems is typically large, and thus large separation between the channel taps can be tolerated that will decrease the overall number of required taps. Note that the hardware can be reduced even more by uniting the feedback block of the emulator for all of the clusters as shown in Fig. 5.5, and thus getting rid of the feedback block accompanied with each cluster. This comes with the price of forcing all the clusters to have the same Variable Attenuation value. This does not offer high flexibility in

controlling each cluster separately. This method isn't recommended since the number of emulated clusters is typically not that large even for outdoor low frequency channels according to the reviewed literature. Thus, the feedback loops that are to be saved are not that effective as compared to the offered flexibility when each cluster has its own feedback loop where there would typically be a few increment in the hardware.
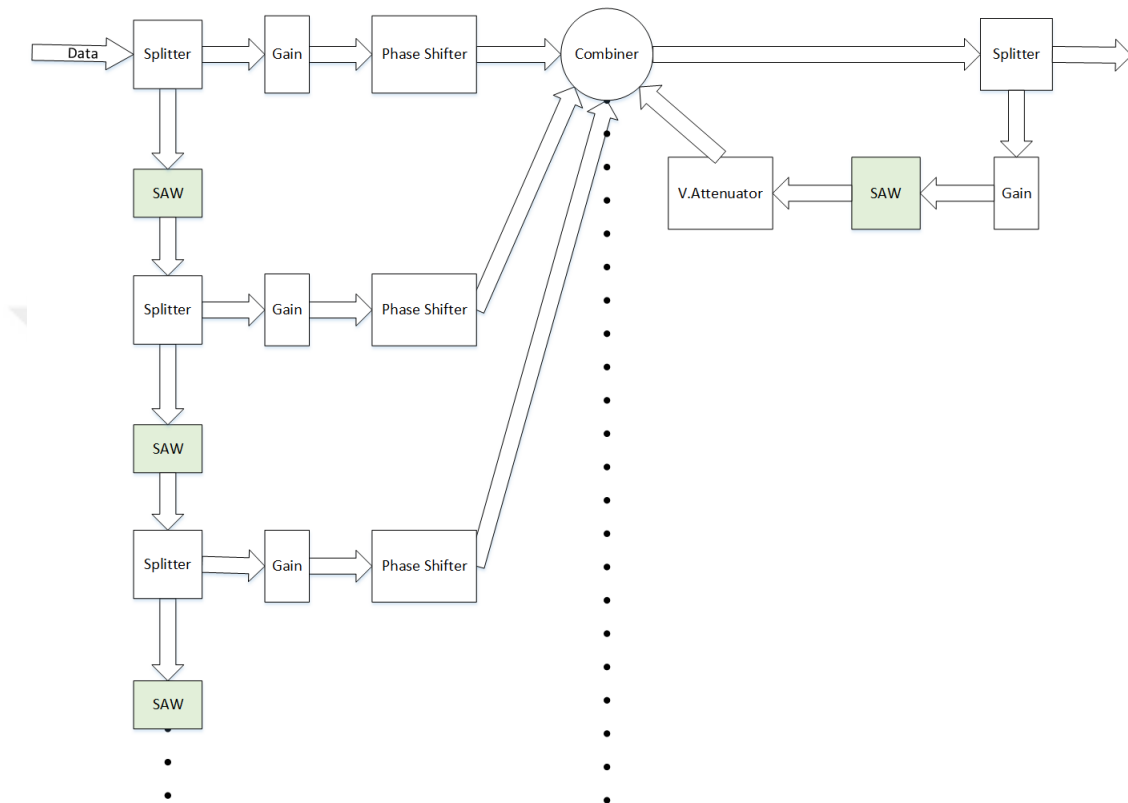

FIGURE 5.5: Illustrative figure that shows the minimum hardware emulation technique for a channel with multiple clusters

Fig. 5.6 shows a 3-taps channel emulated utilizing the cascaded technique. A pattern of 1 followed by a large number of 0s was sent by the generator with Amplitude Shift Keying (ASK) modulation. Note that such a channel is considered to be very frequency selective for the sent signal since the delay between the selected taps is too large as compared to the symbol duration where ISI takes place. However, the chosen symbol rate, and modulation scheme is for the sake of clarifying the channel delay taps on the oscilloscope where the taps are too obvious in the shown figure. The utilized 813-SL140.0M-77A bandpass SAW filter is shown in Fig. 5.7. It offers absolute group delay of 0.78 μsec at a center frequency of 140 MHz, and a group delay variation of up tp 40 nsec among a huge bandwidth of 70 MHz. The filter is characterized by a huge insertion loss of up to

25 dB at its center frequency. Thus, an amplifier is attached with each SAW filter to compensate this significant loss.
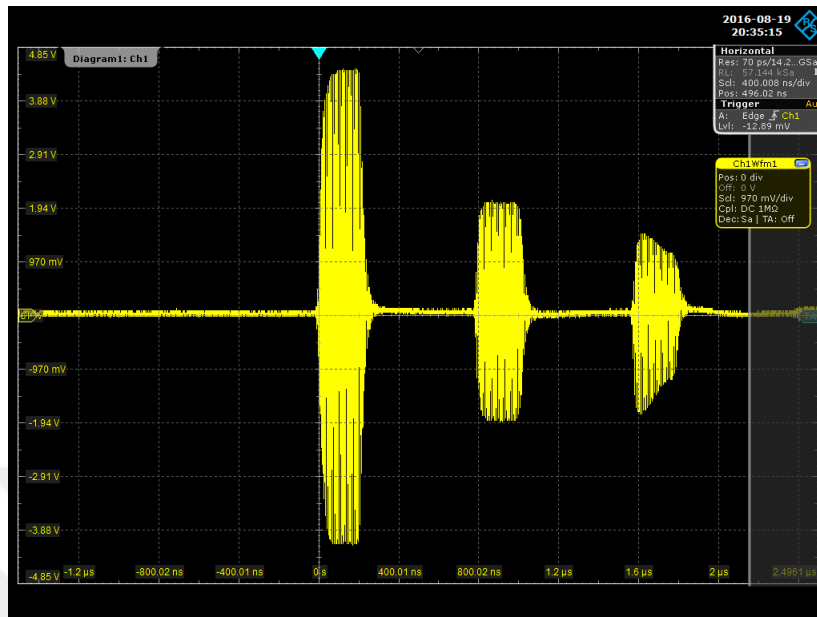

FIGURE 5.6: A 3-taps channel emulated using two SAW filters
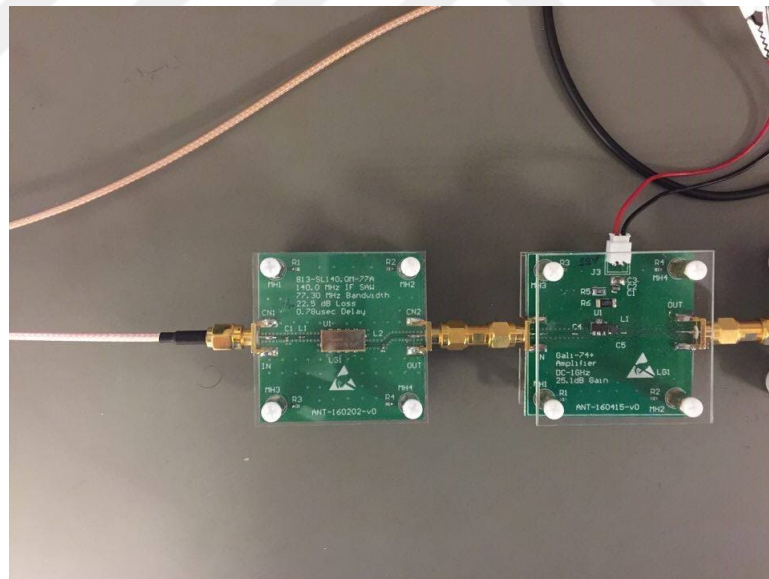

FIGURE 5.7: The utilized lossy SAW filter cascaded by an amplifier to make up for the huge insertion loss caused by the SAW filter

A valid option to increase the flexibility of the delay of the channel taps is by switching the signal between several parallel branches. Each branch is characterized by its delay. However, the offered flexibility is still much lower than the software emulation.

5.2   Doppler Spread

Now that different channel taps have been separated from each other through the uti-lization of SAW filters, it is required to process each tap by its corresponding Doppler spread. The effect of receiving many copies of the sent symbol is represented mathemat-ically by convolution in time domain of the sent data with the channel $h(t, \tau)$ given in equation 2.1. A convolution in the time domain indicates a corresponding multiplication in the frequency domain. The delayed Kronecker delta function taps in the equation are translated as SAW filters in the hardware domain. The Doppler spread as explained earlier indicates a frequency shift. This cannot be represented mathematically as the multiplication of the data with the channel in the frequency domain, but rather a con-volution in the frequency domain that indicates a multiplication in time domain with a time-varying function. This time varying function is represented by the term $c(t)$ in equation 2.1. For the sake of generality, this $c(t)$ is decomposed into a number of $c_n(t)$ factors where n indicates the index of the nth channel tap and it take values from 1 to N. The time variation of the nth channel tap is represented by $c_n(t)$ whose time varia-tion depends the frequency of operation and on the motion scenario of the transmitter, receiver and the surrounding object/s causing the reception of this tap. The taps are received from different angles at the receiver and from different objects moving indepen-dently from each other. Thus, each tap might have its unique Doppler spread model and hence unique $c_n(t)$. It is then required to multiply the nth delayed signal copy with the corresponding $c_n(t)$ of that tap.

As decided earlier, time domain filtering will be the utilized approach in this study. The subscript n will be omitted since the discussion will be for the generation of the Doppler spread waveform for only a single tap. Afterwards, the same concept is applicable for the rest of the taps, each with its own Doppler spread.

Jakes model [22] is one of the most famous models that assumed an isotropic fading channel in which equal powered received multipath signals arrive from all directions or angles of arrival within the same tap. An isotropic scattering Rayleigh fading channel is assumed with an omnidirectional antenna at the receiver. $c(t)$ is then modeled as a Gaussian process $c(t) = c_i(t) + jc_q(t)$. Both $c_i(t)$ and $c_q(t)$ are Gaussian-distributed independent stochastic processes that have the same auto-correlation function (ACF) $R_{c_i,c_i}(\tau) = R_{c_q,c_q}(\tau) = J_0(2\pi f_D \tau)/2$, where f_D is the maximum Doppler frequency in

the continuous domain and $J_o(.)$ is the zeroth-order Bessel function of the first kind [28]. The power spectral density (PSD) associated with either the in-phase or quadrature component of $c(t)$ has the well known Jakes' U-shaped form with independent in-phase and quadrature samples [41]:

$$S_c(f) = \begin{cases} \dfrac{1}{\pi \sqrt{f_D{}^2 - f^2}} & \text{if } |f| < f_D \\ 0 & \text{otherwise} \end{cases} \tag{5.1}$$

Two issues are to be considered for the introduction of the channel effect on a certain tap. Firstly, the power spectrum of each of the quadrature components of the channel fading waveform should follow the desired PSD. Secondly, the distribution of the in-phase and the quadrature phase components of this fading waveform should be Gaussian within the transmitted symbol duration so that the amplitude of the fading waveform follows a Rayleigh distribution. This Rayleigh distribution is the typical case for NLOS and the desired case to be implemented.

If a set of randomly generated samples are independent, then the ACF of this sequence is a single delta function at time zero. This means that the generated sample is only related with itself and has zero correlation with the rest of the samples. This makes the corresponding PSD flat having the same value for all frequencies. Note that the PSD is simply the Fourier transform of the ACF. When an input signal $x[n]$ is passed through a filter with frequency response $H(e^{jw})$ then the output $y[n]$ has the power spectrum $S_{yy}(e^{jw}) = S_{xx}(e^{jw}) * |H(e^{jw})|^2$ where $S_{xx}(e^{jw})$ is the power spectrum of the input signal. Therefore, to have a signal with a certain PSD, a sequence of independent samples can be passed through an SSF whose amplitude frequency response $|H(e^{jw})|$ is the square root of the desired PSD. Thus, the problem reduces to designing a filter with a certain amplitude response. Note that there are no restrictions on the phase response of the output signal as the restriction is only on the amplitude response. Hence, the filter does not have to be a linear phase filter offering flexibility in its design.

More than one reference were cited in the literature survey concerning designing a filter with an extremely narrow passband and sharp cutoff. The requirement of an extremely narrow passband filter is due to the fact that the data is being multiplied with the generated channel fading waveform in a processor via a software. This means that the sampling rate of the data and the channel have to match in order to be able to carry

out this multiplication. The Doppler spread is typically very small as compared to the frequency of operation in most of the real cases; i.e. $f_D << f_c$ where f_c is the carrier frequency. Therefore, in the digital domain, F_D (the maximum Doppler frequency shift in the digital domain) has to be very small as compared to the data sampling rate making the design of the filter in the digital domain a challenging task. In MATLAB, the filter design functions follow a normalization where the frequencies to be entered should be from -1 to 1 where 1 corresponds to the Nyquist frequency that is half the sampling rate. In digital signal processing, the convention adopted is that digital frequencies vary from -1/2 to 1/2 where 1/2 corresponds to the Nyquist rate. Therefore, the maximum Doppler digital frequency that can be used in MATLAB F_D' is given by the equation:

$$F_D' = 2 * F_D \tag{5.2}$$

If the sampling rates of the channel fading waveform and the data should match to be multiplied in the baseband, then F_D' should typically be much less than 1. Hence, a large number of filter coefficients is required to meet the amplitude response specification with a good accuracy, increasing the SSF complexity. Therefore, these cited papers are concerned with solving that problem. However, proposed in this study is the multiplication of the channel fading waveform with the data in the RF domain (bandpass). Therefore, a microcontroller is used only for the generation of the channel fading waveform where this waveform will be processed and fed as a control signal to a variable attenuator that changes the amplitude level of the data accordingly. Hence, the multiplication does not take place inside the microcontroller itself. This channel fading waveform is generated in the microcontroller by generating sequence of independent samples and passing it through an SSF whose coefficients are previously calculated via MATLAB. Note that the sampling rate of the channel fading waveform depends on the crystal frequency of the used microcontroller itself and the number of operations within each code loop that produces a fading sample. After specifying certain number of the SSF coefficients, and by knowing the extra processing done for the fading waveform inside the microcontroller code, the duration of the microcontroller code loop is determined exactly. By knowing the sampling rate, and with the previous knowledge of the desired f_D to be modelled, F_D value can be derived through:

$$F_D = T_s * f_D \tag{5.3}$$

where T_s is the sampling period that the microcontroller spends in one loop to generate a single fading sample.

No upsampling is required to be done within the microcontroller since the multiplication is not carried out in it. Thus, F'_D typically will not have to be that small in order to result in the desired f_D and hence, less number of filter coefficients are required to approximate the desired amplitude response of the filter. As mentioned earlier, IIR filter gives the desired amplitude response with much less coefficients than an FIR filter. The Matlab function `iirlpnorm` designs an IIR filter that result into the given specified amplitude response. After the quantization of the filter coefficients returned by this function from floating-point to fixed-point, the filter stability has to be checked before typing those coefficients in the microcontroller code.

As for the distribution issue, and as mentioned before, the amplitude of the channel fading waveform should follow Rayleigh distribution for the NLOS case within the duration of each transmitted symbol. Prior to 4G systems, increasing the data rate used to come with the expense of increasing the transmitted symbol rate. On the opposite side, new OFDM systems as well as systems beyond 4G are expected to employ the multicarrier modulation technique where achieving a high data rate is not a result of decreasing the transmitted symbol duration but rather through the transmission of many orthogonal carriers in parallel with elongated duration. The purpose of increasing the transmitted symbol duration is to combat the channel frequency selectivity. Each of those orthogonal channels occupy much less bandwidth as compared to the single carrier modulation scheme. This makes the channel approximately flat within this small bandwidth and hence no complex equalization is needed at the receiver side, which is required in the case of single-carrier systems with high data rate. In time domain, single-carrier systems symbol duration is typically too small as mentioned before. Within this small duration small number of channel fading waveform samples is being generated. Whereas for multi-carrier systems, larger number of fading waveform samples is generated since the symbol duration is much longer. Therefore, for the single-carrier systems, the generated sequence of independent samples that are to be passed through the SSF should follow a Gaussian distribution in order to result into a Rayleigh distributed amplitude. Note that the SSF preserves the Gaussian distribution of the input. Whereas, for systems whose symbol duration is relatively long, this generated sequence can follow *any* distribution and the resulting sequence at the output of the SSF will still follow Gaussian distribution. This

observation is based on experiment. One possible interpretation is the applicability of the central limit theorem where a very large number of samples are generated within a single symbol. These samples, will eventually follow a Gaussian distribution when the symbol duration is large enough. This observation is crucial since it makes the generation of the Rayleigh channel fading waveform much simpler for OFDM systems where the on-shelf "uniform" random number generators that already exist in microcontroller libraries can be utilized without having to bother with transforming this independent uniformly distributed random sequence into Gaussian before passing it through the SSF. It is widely known that generating a sample sequence with a desired distribution can be achieved by transforming a sequence of uniformly distributed samples along the interval [0,1] with the inverse cumulative distribution function (CDF) of that distribution. Unfortunately, there is no closed form expression for the inverse CDF function of the Gaussian distribution and hence there exist many algorithms for generating a Gaussian sequence out of uniform sequences such as the famous Box-Muller transform as well as approximations for the inverse CDF function. However, implementing those algorithms in the microcontroller code will result into a longer code loop duration and hence a smaller sampling rate. This can be avoided if the tested system has a long enough symbol duration. Note that these algorithms are based on the presence of a uniformly distributed sequence that can then be transformed into a Gaussian one. Uniform random number generators exist vastly even in the simplest microcontrollers libraries unlike other distributions that are usually generated by a more sophisticated resources such as MATLAB.

Shown in Fig. 5.8 and Fig. 5.9 are the histogram of the uniformly distributed input samples and the histogram of the output samples from the SSF respectively. It is very clear that the output has a Gaussian distribution though the input has a uniform one. Note that the number of samples is too large.
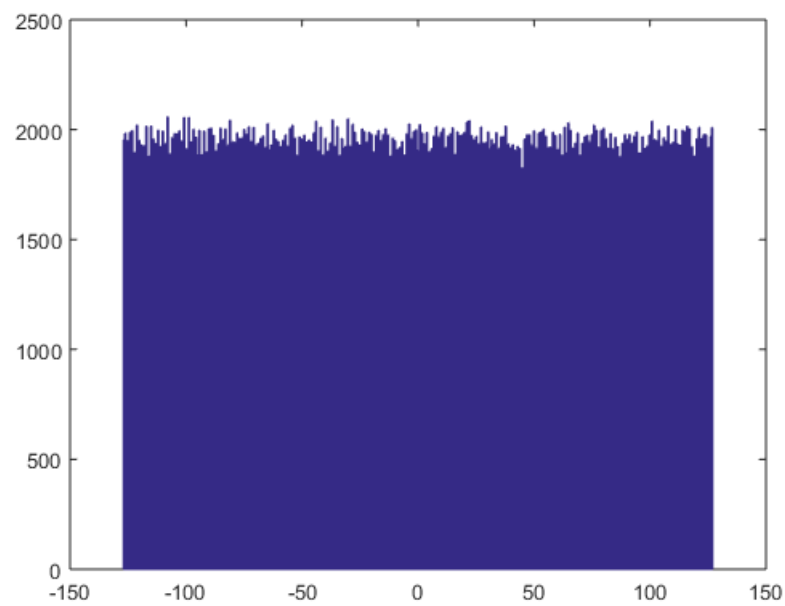
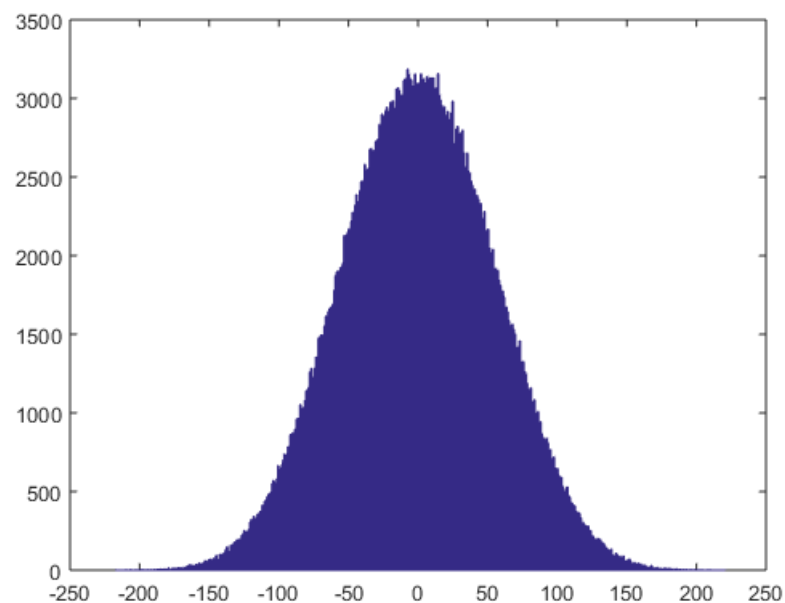FIGURE 5.8: Histogram of the uniformly distributed input to SSF

FIGURE 5.9: Histogram of the Gaussian distributed output from the SSF when the input is uniformly distributed with large number of samples

Shown in Fig. 5.10 and Fig. 5.11 are the histogram of the Poisson distributed input samples and the histogram of the output samples from the SSF respectively. It is very clear that the output has a Gaussian distribution though the input has a Poisson one. Note that the number of samples is still too large. Thus, it is proven by experiment

that the output from the SSF will have a Gaussian distribution no matter what the distribution of the input is under condition that large number of samples are being spanned.
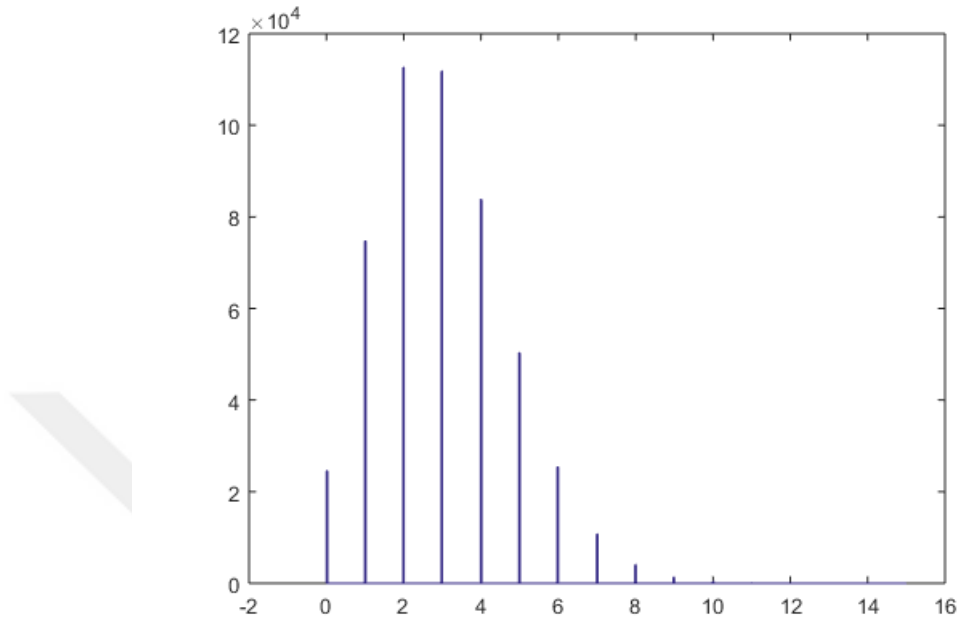

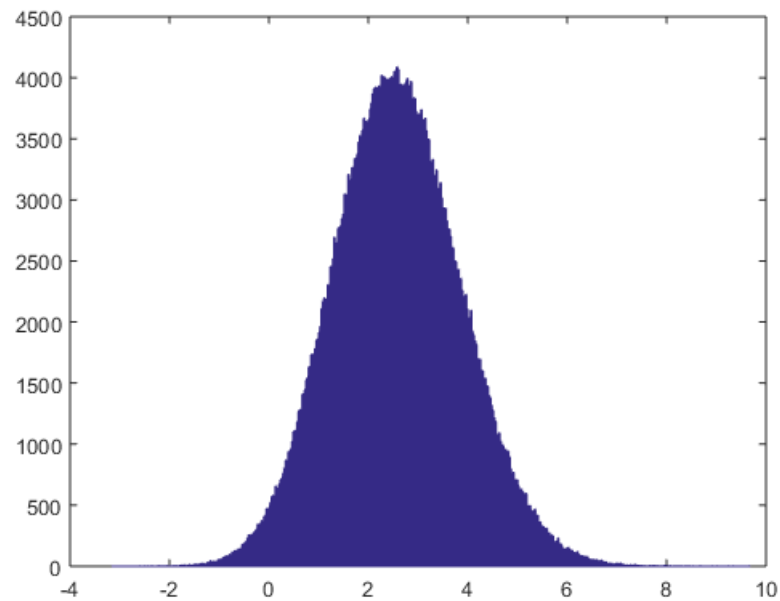FIGURE 5.10: Histogram of the Poisson distributed input to SSF

FIGURE 5.11: Histogram of the Gaussian distributed output from the SSF when the input is Poisson distributed with large number of samples

Note that in some cases, and depending on the speed of the used processing hardware and the tested communication system, T_s might be very large that it might even be longer than the transmitted symbol duration. In such cases, the distribution of the independent samples entering the SSF should still follow Gaussian distribution so that the Amplitude distribution of the sent message that contains several symbols is still Rayleigh.

5.2.1 Doppler Implementation blocks explanation

Shown in the following two figures are two different approaches to introduce predefined Doppler spread effect on each channel tap. Note that each channel tap may have its unique Doppler spread and hence both of the approaches can be implemented in emulating the same channel where each approach will be adopted on a separate channel tap.

The mathematical representation of the Doppler spread effect on a channel tap is as follows. Consider one of the channel taps in the RF domain that can be represented as $A+jB$ representing the two quadrature components of one copy (tap) of the sent signal, it is required to multiply it with the Doppler fading waveform represented by c_i+jc_q. Thus we have

$$(A + jB) * (c_i + jc_q) = ((A + jB) * (c_i)) + (j(A + jB) * (c_q)). \tag{5.4}$$

The right had side (RHS) of the equation requires the splitting of the data to two different branches where one of them will be phase shifted by 90^0. Note that this is possible because the data is in the RF domain where the inphase component A and the quadrature component B exist together in the same cable. This is in contrast with the components of the fading waveform c_i and c_q, which are in the baseband and thus, each one is in a separate branch. However, after splitting the data and phase shifting one of the branches, the next step is to multiply the unshifted branch with $|c_i|$ and the shifted branch with $|c_j|$ as indicated by the RHS of the equation. The sign of c_i and c_j is translated in hardware as a 180^0 phase shift of the resulting multiplied output. Therefore, a switch is required to route the output whether toa 180^0 phase shifter or not. The switch takes its control from a pin in the same microcontroller generating the corresponding waveform. Finally, both of the "sign" branches are added together through a combiner to result into one of the two halves of the RHS of the equation. The

same operation is done for the other branch that only has a phase shift difference to give the other half of the RHS of the equation. Finally, the two "quadrature" branches are combined together to result into the signal tap affected by the desired Doppler spread according to the equation. The explained switch approach is shown in Fig. 5.12. The use for an attenuator as a multiplication element will be discussed

Another implementation is shown in Fig. 5.13. This can be utilized in the scarcity of switches. It depends on the separation of the fading waveform c as follows:

$$c(t) = c^+(t) + c^-(t). \tag{5.5}$$

At a certain time instant t, one of the positive branch, $c^+(t)$, or the negative one, $c^-(t)$, should be equal to $c(t)$ while the other should ideally be equal to zero. Thus, the utilized attenuators should be capable of achieving very large attenuation value in order to suppress the zero branch since no switches are used here. The same microcontroller should be used to control the attenuation of both c attenuators from two different ports. For example, if c of a certain fading sample is positive, then the multiplication should be done through the c^+ attenuator as explained earlier while the c^- attenuator should be fed with the voltage value that leads to the maximum attenuation. Using low attenuation attenuators will lead to an undesired distortion that is not related to the channel effects desired to be emulated. This is because one of the sign branches affects the data at the same instant of getting the data from the other branch. Hence, the switch method is more preferable.
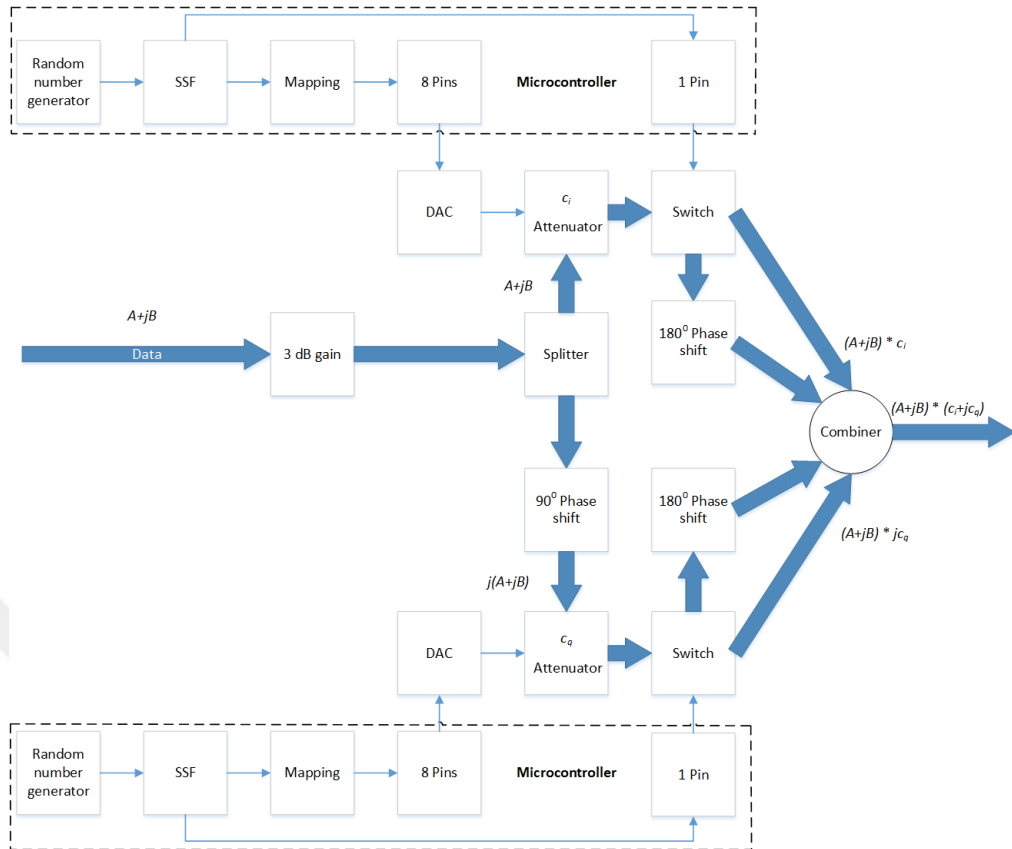
FIGURE 5.12: Doppler spread introduction technique utilizing switches
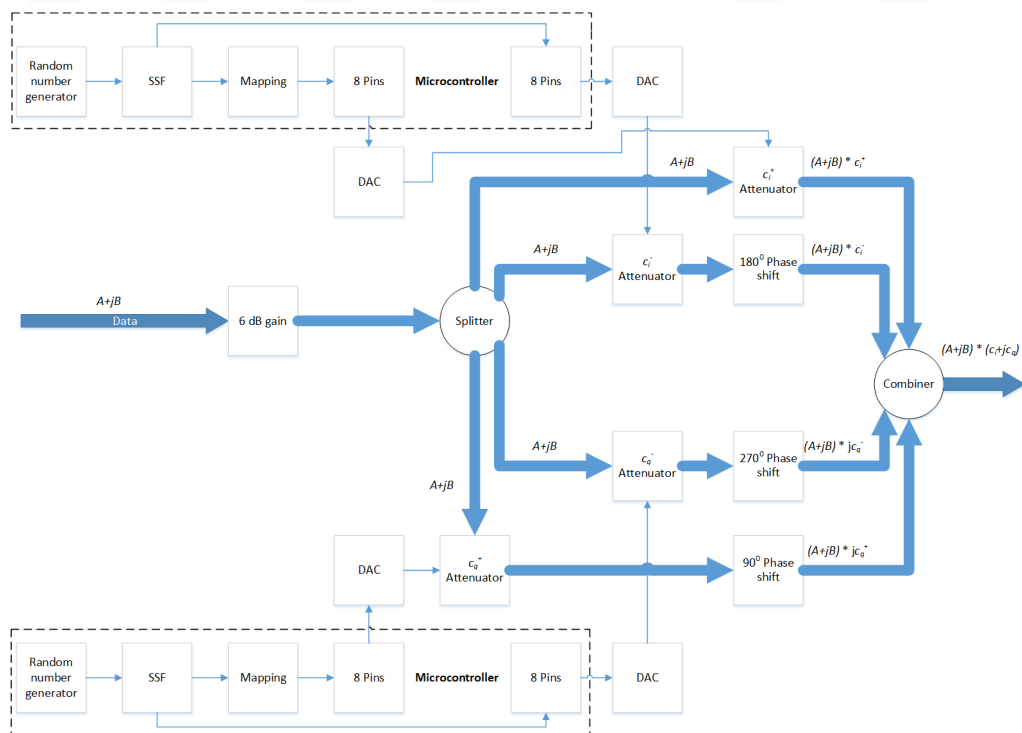

FIGURE 5.13: Doppler spread introduction technique utilizing high-attenuation attenuators

5.2.2   Doppler Implementation issues

According to both of the figures, two independent sequences of randomly generated independent samples are passed through the SSF filter whose coefficients were previously calculated using MATLAB as mentioned before. If the absolute value of the sample is greater than one, an amplifier has to be used for the multiplication of the sample with the data while an attenuator should be used if less than one. This would require another switch in order to route the signal whether to the amplifier or the attenuator. This is in addition to the switch used for the sake of the sign of the sample as explained earlier. In this case, each microcontroller branch will be required to control two switches, attenuator and an amplifier. Analog controlled variable gain elements (amplifiers and attenuators) are preferable to the digital ones. The reason behind that is to be able to get a continuous fading signal. According to the data sheet of the used gain element, a mapping function should be inserted in the microcontroller code that maps the desired absolute $|c|$ value to the corresponding input voltage V that should be entered as a control signal to the gain element. This can be simply done by polynomially fitting $|c|(V)$ and then calculating the inverse function to have it in the form of $V(|c|)$.

In reality, there are limitations to the attenuation/amplification values of any gain element. Therefore, it is hard to translate the absolute c value into the exact V level that gives the corresponding attenuation/amplification. Instead, only one gain element can be utilized (attenuator) where only the relativity between the resulting samples from the SSF are taken into consideration. This is done by mapping the resulting stream from the SSF to the region of operation of the selected attenuator. For example, $|c|=0.25$ will not have to correspond to V resulting into 6dB attenuation. It can be assigned any attenuation level in the microcontroller as long as $|c|=0.125$ is attenuated by 3dB more. Hence, only the relativity between the samples are taken into account, not their absolute values. However, the absolute level can be taken care of in the main gain element of the tap that already exists as shown in Fig. 5.2. This method has several advantages. The exemption of constraining a certain $|c|$ value to a certain attenuation value gives the flexibility to work in the most appropriate region of the attenuator (linear region). The reason behind preferring the linear region of the attenuator is explained in the next paragraph. Another advantage is the saving of extra computation in the microcontroller

for controlling 2 switches, attenuator, and an amplifier. Only one switch and an amplifier are controlled. This also lead to the hardware saving since the gain element of the channel tap already exists in any case. Only the absolute amplification/attenuation value of the tap will have to be adjusted.

Many microcontrollers have digital output ports only. To feed the attenuator with an analog continuous signal as discussed before, we are then left with two options. The first is to utilize the Pulse Width Modulation (PWM) technique. This offers high flexibility in achieving any desired V voltage to get the desired attenuation. However, the drawback of this option is the time consumption that will lead to an enormous sampling rate reduction. Therefore, we are left with the second option where the output is taken from the digital output pins of the microcontroller and then passed through a DAC and finally fed to the attenuator. Though this approach does not have the sampling rate reduction problem, it implies limitation on the possible V values to be acquired within the whole scale range of the attenuator, which is from 0 to 5 volts in many of the commercially available attenuators. The number of attainable V levels is given by

$$\#V = 2^{\#pins}. \tag{5.6}$$

where $\#pins$ is the number of digital pins from which the output is taken and then converted to an analog signal by the use of DAC. These attainable levels are distributed linearly among the chosen range. To deal with this issue, it is desired to utilize an attenuator whose input control voltage levels are well distributed among the whole attenuation range. This is in order to make the maximum use of the available V levels and not to waste so many of them in regions where many levels correspond to nearly the same attenuation level while other attenuation regions are served by much less number of V levels. Note that the DAC can be manipulated in order to distribute the levels linearly in any chosen range. Thus, it is not mandatory to use the whole range of the attenuator control voltage. In this case, the offered V levels will be used in the region where fairness between different attenuation levels becomes satisfying.

5.2.3   Results from Doppler block

Shown in Fig. 5.14 is the PSD of the fading waveform that resulted from the used SSF before the mapping to V values. The simulation was done via MATLAB to validate

that the spectrum of the output of the SSF has the desired U shape of Jakes model. The used SSF structure is shown in Fig. 5.15 and the coefficients are as follows: the denominator coefficients are $a_1 = 1.1976$, $a_2 = -1.5639$, $a_3 = 0.7525$, $a_4 = -0.282$, while the numerator coefficients are $b_0 = 0.1104$, $b_1 = 0.1579$, $b_2 = 0.2364$, $b_3 = 0.1579$, $b_4 = 0.1104$. These coefficients are the approximated coefficients got from MATLAB utilizing the `iirlpnorm` function for $F_D = 0.4$. Note that the denominator coefficients have inverted sign values as compared to those got from MATLAB as it follows the assumption that they are multiplied with a negative sign.
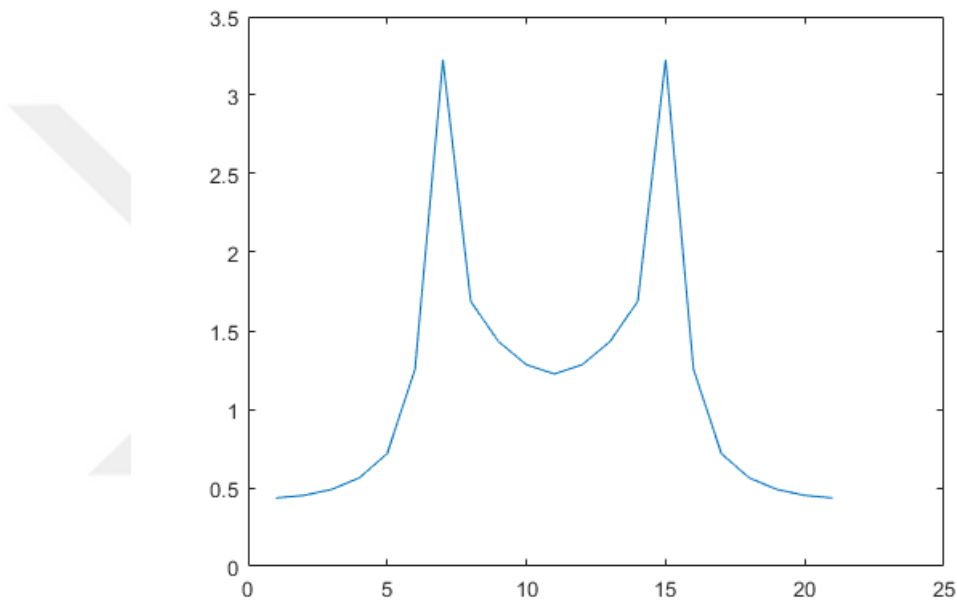

FIGURE 5.14: Absolute FFT of the fading waveform resulting from microcontroller
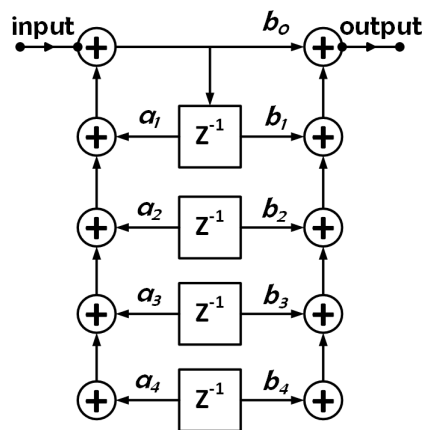

FIGURE 5.15: Utilized SSF

5.3   Chapter Conclusion

A predefined hardware channel emulator at 140 MHz is proposed, implemented, and tested. SAW filters are utilized as delay elements to achieve large delay values that typically accompany such low frequencies in outdoor environments. Multiple clusters channels with large number of taps per cluster are modelled through the cascaded and the feedback technique. Feedback technique serves in saving hardware resources where every single channel tap will no more need a separate dedicated branch. This comes with the expense of loosing control on the fed-back taps due to the dependence of each tap on the previous one. According to the number of taps, the advantages and the disadvantage of the feedback technique have to be compromised to get the best solution. Doppler effect was efficiently introduced to the signal in the RF domain by the use of SSF - whose coefficients are previously calculated on MATLAB- to filter independent samples in time domain. This led to a great advantage of saving computational complexity that would have been needed due to the upsampling of the SSF if the time-domain filtering was to be introduced in the baseband. Also by using fast enough processor and with systems of large transmitted symbol duration, the input sequence to the SSF ought not to be Gaussian in order to result into a Gaussian sequence at the output. This might be due to the applicability of the central limit theorem that would result into a Gaussian distribution at the output while the input might follow *any* distribution. This would save extra computation and offer higher sampling rate. The proposed emulator is generally simple, cost-efficient. Moreover, it can be used to assess the performance of communication systems for long enduring time due to the time-domain filtering approach utilized with the SSF. This because the memory requirement and the block-oriented nature of the frequency-domain filtering is avoided. Therefore, the advantage of time-domain filtering is achieved while the computational complexity expense was avoided by introducing the effect in the RF domain.

Chapter 6

Conclusion and Future Work

The process of assessing the performance of a newly developed communication product through actual measurements is a time-consuming and expensive process. It might even be inapplicable in some cases. Thus, there comes the need to perform this testing in a laboratory where the wireless channel effect is introduced to the signal in RF domain or in processors via software codes. In order to imitate the channel effect, the behavior of the channel should be accurately studied to be able finally to produce a model that describe the channel dynamics precisely. This precision shall increase as the data rate of the tested product increase due to the corresponding increase in the vulnerability of the signal to a certain channel. Modelling the channel directional attributes is crucial in the testing of MIMO systems. This thesis provided a general explanation for the wireless channel behavior. A quick survey for different software models and hardware emulators for predefined channels were also introduced. A directional software FM channel model is developed by the authors for hilly outdoor environments. The model is based on previously existing models where different parameters were adapted to better fit the FM band. A hardware emulator is also implemented in this study for a predefined channel. The proposed emulator has many advantages. It can be used in ongoing testing of products. This is because the the generation of the correlated fading samples is carried out by the SSF that performs the filtering of independent samples in time domain not the frequency domain. The frequency domain filtering has the drawback of specific memory requirements and block-oriented nature that does not help in performing tests for large duration. However, the time-domain filtering may result in huge computational complexity due to the design of extremely narrow-band filters since the Doppler shift is typically

much smaller than the frequency of operation. This is avoided by the introduction of the Doppler effect to the signal in the RF domain where the processing hardware component is only used for the generation of the fading samples waveform. The multiplication of the symbol with the fading waveform is done in an attenuator. Besides, no undesired distortions are introduced to the signal due to the down and up conversions that take place in software simulators. Thus, this emulator could achieve the advantages of different techniques.

As for the MIMO case, the signal will have to pass through many channels in parallel. The characteristics of each one should be predefined to emulate it in hardware. The same proposed technique might be used to emulate each of them and the receiver will get the resultant of the signal processed by the each of those channels via different ports (antennas). Shown in Fig. 6.1 is a structure of a MIMO channel where two inputs from two different antennas are being sent on the same frequency at the same time and the two processed inputs are received from two ports. Each input is to be determined through complex processing of the two received outputs.
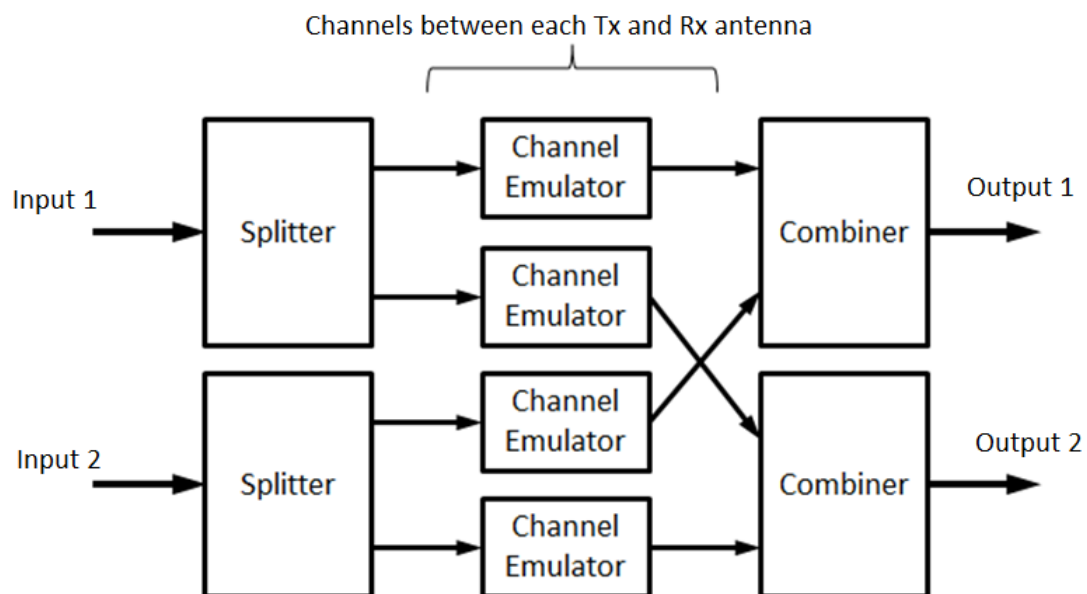

FIGURE 6.1: Structure of a MIMO channel emulator

Bibliography

[1] 2016. URL `http://iwcmediaecology.pbworks.com/w/page/8480806/Guglielmo%20Marconi`.

[2] 2016. URL `http://www.ee.nthu.edu.tw/~yhhuang/Communication%20DSP%20and%20IC.htm`.

[3] Hindawi, 2016. URL `http://www.hindawi.com/journals/ijap/2010/735434/fig7/`.

[4] Z.Pedrini, 2016. URL `http://www.telecomhall.com/what-is-isi-inter-symbol-interference-in-lte.aspx`.

[5] C.Chen, 2015. URL `http://princetoninnovation.org/magazine/2015/12/09/redshift-universes-doppler-effect/`.

[6] A.Aitalieva. VHF Channel Modeling for Wireless Sensor Networks. Master's thesis, Gebze Technical University, Gebze, Kocaeli, Turkey, 2015.

[7] 2016. URL `http://www.token.com.tw/pdf/saw/saw-devices.pdf`.

[8] Clear Doubts, 2016. URL `http://www.cleardoubts.com/technology/what-is-1g-or-first-generation-of-wireless-telecommunication-technology/`.

[9] G.J. Foschini and M.J. Gans. On limits of wireless communications in a fading environment when using multiple antennas. *Wireless personal communications*, 6 (3):311–335, 1998.

[10] A.F. Molisch, H. Asplund, R. Heddergott, M. Steinbauer, and T. Zwick. The COST259 directional channel model-part I: Overview and methodology. *IEEE Transactions on Wireless Communications*, 5(12):3421–3433, 2006.

[11] A.A.M. Saleh and R.A. Valenzuela. A Statistical Model for Indoor Multipath Propagation. *Selected Areas in Communications, IEEE Journal on*, 5(2):128–137, February 1987. ISSN 0733-8716. doi: 10.1109/JSAC.1987.1146527.

[12] H. Asplund, A.A. Glazunov, A.F. Molisch, K.I. Pedersen, and M. Steinbauer. The COST 259 Directional Channel Model - Part II: Macrocells. *Wireless Communications, IEEE Transactions on*, 5(12):3434–3450, December 2006. ISSN 1536-1276. doi: 10.1109/TWC.2006.256967.

[13] M. Zhu, G. Eriksson, and F. Tufvesson. The COST 2100 channel model: Parameterization and validation based on outdoor MIMO measurements at 300 MHz. *Wireless Communications, IEEE Transactions on*, 12(2):888–897, 2013.

[14] A. Webster. Modeling and Measurement Techniques for 5GHz Wireless LAN Transceivers. M.s. thesis, University of South Florida, 2004.

[15] A. Algans, K.I. Pedersen, and P.E. Mogensen. Experimental analysis of the joint statistical properties of azimuth spread, delay spread, and shadow fading. *Selected Areas in Communications, IEEE Journal on*, 20(3):523–531, 2002.

[16] T.S. Rappaport. *Wireless Communications: Principles and Practice*. Wireless Communications Series. IEEE, 1996. ISBN 9780780311671. URL `https://books.google.com.tr/books?id=5weyKAAACAAJ`.

[17] T.S. Rappaport, S.Y. Seidel, and R. Singh. 900-MHz multipath propagation measurements for US digital cellular radiotelephone. *Vehicular Technology, IEEE Transactions on*, 39(2):132–139, 1990.

[18] A. Zogg. Multipath delay spread in a hilly region at 210 MHz. *IEEE transactions on vehicular technology*, 36(4):184–187, 1987.

[19] A. Aitelieva, G. Celik, and H. Celebi. Ray tracing-based channel modelling for VHF frequency band. In *Signal Processing and Communications Applications Conference (SIU), 2015 23th*, pages 1385–1388, May 2015. doi: 10.1109/SIU.2015.7130100.

[20] S. Güzelgöz, S. Yarkan, and H. Arslan. Investigation of time selectivity of wireless channels through the use of RVC. *Measurement*, 43(10):1532–1541, 2010.

[21] RH Clarke. A statistical theory of mobile-radio reception. *Bell system technical journal*, 47(6):957–1000, 1968.

[22] W.C. Jakes and D.C. Cox. *Microwave mobile communications*. Wiley-IEEE Press, 1994.

[23] Y.R. Zheng and C. Xiao. Simulation models with correct statistical properties for Rayleigh fading channels. *Communications, IEEE Transactions on*, 51(6):920–928, 2003.

[24] M.F. Pop and N.C. Beaulieu. Design of wide-sense stationary sum-of-sinusoids fading channel simulators. In *Communications, 2002. ICC 2002. IEEE International Conference on*, volume 2, pages 709–716. IEEE, 2002.

[25] A. Alimohammad, S.F. Fard, B.F. Cockburn, and C. Schlegel. An improved SOS-based fading channel emulator. In *Vehicular Technology Conference, 2007. VTC-2007 Fall. 2007 IEEE 66th*, pages 931–935. IEEE, 2007.

[26] C. Komninakis. A fast and accurate Rayleigh fading simulator. In *Global Telecommunications Conference, 2003. GLOBECOM'03. IEEE*, volume 6, pages 3306–3310. IEEE, 2003.

[27] J. I. Smith. A computer generated multipath fading simulation for mobile radio. *IEEE Transactions on Vehicular Technology*, 24(3):39–40, Aug 1975. ISSN 0018-9545. doi: 10.1109/T-VT.1975.23600.

[28] A. Alimohammad, S.F. Fard, and B.F. Cockburn. Filter-based fading channel modeling. *Modelling and Simulation in Engineering*, 2012:3, 2012.

[29] D.J. Young and N.C. Beaulieu. The generation of correlated Rayleigh random variates by inverse discrete Fourier transform. *Communications, IEEE Transactions on*, 48(7):1114–1127, 2000.

[30] K. Yip and T. Ng. Efficient simulation of digital transmission over WSSUS channels. *Communications, IEEE Transactions on*, 43(12):2907–2913, 1995.

[31] R.A. Goubran, H.M. Hafez, and A.U.H. Sheikh. Implementation of a real-time mobile channel simulator using a DSP chip. *Instrumentation and Measurement, IEEE Transactions on*, 40(4):709–714, 1991.

[32] A. Alimohammad, S.F. Fard, B.F. Cockburn, and C. Schlegel. A compact single-FPGA fading-channel simulator. *Circuits and Systems II: Express Briefs, IEEE Transactions on*, 55(1):84–88, 2008.

[33] L.B. Jackson. Chapter 11/Quantization Effects. *Digital Filters and Signal Processing, 2d Edition, Kluwer Academic Publishers*, pages 297–340, 1989.

[34] M. Karabacak, A. Şahin, and H. Arslan. RF DOMAIN CHANNEL EMULATION TECHNIQUES WITH SAW FILTERS. In *Conference on Communications Technologies and Software Defined Radio (SDR - WInnComm)*, volume 1, pages 1–5. Wireless Innovation Forum, 2013.

[35] E. Damosso. *Digital Mobile Radio Towards Future Generation Systems, COST 231 Final Report*. EUR 18957, 1999.

[36] M.L. Meeks. VHF propagation over hilly, forested terrain. *Antennas and Propagation, IEEE Transactions on*, 31(3):483–489, May 1983. ISSN 0018-926X. doi: 10.1109/TAP.1983.1143066.

[37] P.Pathania, P.Kumar, and S.B. Rana. A Modified Formulation of Path Loss Models for Broadcasting Applications. *International Journal of Recent Technology and Engineering (IJRTE)*, 3(3):44–54, July 2014. ISSN 2277-3878.

[38] L.J. Greenstein, V. Erceg, Y.S. Yeh, and M.V. Clark. A new path-gain/delay-spread propagation model for digital cellular channels. *Vehicular Technology, IEEE Transactions on*, 46(2):477–485, May 1997. ISSN 0018-9545. doi: 10.1109/25.580786.

[39] H. Hofstetter, A. F. Molisch, and M. Steinbauer. Implementation of a COST 259 geometry based stochastic channel model for macro and micro cells. *in Proc. EPMCC*, Feb. 2001.

[40] B.M. Alves, L.L. Mendes, D.A. Guimaraes, and I. Gaspar. Performance of GFDM over Frequency-Selective Channels. In *Proc. International Workshop on Telecommunications*, October 2013.

[41] R.H. Clarke and W.L. Khoo. 3-D mobile radio channel statistics. *IEEE Transactions on Vehicular Technology*, 46(3):798–799, 1997.